

Modellering av blodsukkerdynamikk

Marianne Myhre

Master i teknisk kybernetikk (2-årig)

Innlevert: juli 2013

Hovedveileder: Steinar Sælid, ITK

Norges teknisk-naturvitenskapelige universitet
Institutt for teknisk kybernetikk

Abstract

For persons diagnosed with diabetes mellitus, measuring the blood glucose level is important for the insulin administration. Conventional glucose measurement methods are both uncomfortable and not always reliable. Therefore, alternative methods for glucose measurement are under development. This work, in cooperation with Prediktor AS, was about studying a mathematical model describing the glucose metabolism in the human body. The glucose model is intended to be used in a non-invasive glucose measurement device, where the glucose model is supposed to be used in a Kalman filter for glucose level prediction. Different glucose metabolism models were studied, and a literature review was given. A model was chosen, which roughly seemed to predict the blood glucose level when compared to real glucose data.

The model parameters are already found in the literature, but in order to calibrate the model, the identification properties of the model were studied. The analysis showed that parameters p_1 , p_2 , T_d , α , β and k_{emp} had a certain influence on the glucose output, and were not strongly correlated. However, the choice of parameter vector was not too obvious. Therefore, an algorithm was used to find a suitable parameter vector. Because the algorithm needed real glucose data, real glucose data was collected. Because the collected data did not contain enough information, the algorithm failed to find a suitable parameter vector. For this reason, an optimal experiment was designed, and real glucose data was again collected, in order to use the algorithm and to check if optimal parameter values could be found. The collected data revealed unmodeled dynamics in the chosen glucose model. Therefore, the algorithm in question could not be used, and parameter identification could not be performed. The importance of the unmodeled dynamic should be considered. The chosen model may need to be changed.

Contents

1	Project overview	1
1.1	Diabetes	1
1.2	Insulin administration	2
1.3	Continuous glucose monitoring	3
1.4	Aim of the project	4
2	Literature study	7
2.1	Introduction	7
2.2	Theory	8
2.2.1	<i>Glucose metabolism in a healthy person</i>	8
2.2.2	<i>Glucose metabolism in a diabetic</i>	10
2.3	Minimal model approach	10
2.3.1	<i>Oral glucose intake</i>	11
2.3.2	<i>Pancreatic production</i>	11
2.3.3	<i>Effect of physical activity</i>	11
2.3.4	<i>Subcutaneous insulin injection</i>	12
2.4	Maximal model approach	12
2.4.1	<i>Meal simulation model</i>	13
2.4.2	<i>Model at molecular level</i>	13
2.4.3	<i>Oscillatory insulin secretion</i>	14
2.5	Parameter identification techniques	14
3	Glucose metabolism model	17
3.1	Choice of model	17
3.2	Simulation of the glucose model	22
3.2.1	<i>Simulation for a healthy person</i>	22
3.2.2	<i>Simulation for a healthy person with Kalman filter</i>	24
4	Identifiability analysis	29
4.1	The system identification problem	29
4.2	Identifiability analysis theory	31
4.2.1	<i>Sensitivity-based analysis</i>	31
4.2.2	<i>Practical identifiability analysis</i>	34
4.3	Identifiability analysis of the glucose model	37
4.3.1	<i>Ranking of parameters with different experiments</i>	37
4.3.2	<i>Calculating the covariance matrix</i>	41

4.3.3	Comparing different parameter vector by using the Fishers Information Matrix	43
4.4	Summary	46
5	Calibration and choice of parameter vector based on real glucose data	49
5.1	RDE criterion	49
5.1.1	Parameter estimation methods	51
5.1.2	Collecting glucose data	51
5.1.3	RDE algorithm for the glucose model	52
5.2	Optimal experimental design	54
5.2.1	Numerical solution to the optimal experimental design	55
5.2.2	Design of experiment	57
6	Discussion of results and conclusion	61
6.1	Discussion	61
6.2	Conclusion	61
	References	63
	Appendix	67

List of Figures

1.1	Continious blood glucose sensor with insulin pump	4
2.1	Glucose metabolism process	8
2.2	Insulin control	9
2.3	Example of subcutaneous insulin kinetics	12
3.1	Insulin level	23
3.2	Level of glucose through the digestive system	24
3.3	Real and estimated blood glucose	24
3.4	Extended Kalman filter loop	26
3.5	Real and simulated blood glucose with Kalman filter	27
4.1	The parameter identification process	30
4.2	Sensitivity for parameters 1 to 4	39
4.3	Sensitivity for parameters 5 to 8	39
4.4	Sensitivity for parameters 9 to 12	40
4.5	Sensitivity for a diabetic type 1 person	40
5.1	Real and simulated blood glucose level	50
5.2	Real and simulated blood glucose level	52
5.3	Optimal experimental design loop	55

5.4	CVP and constant input	56
5.5	Optimal experiment	58
5.6	Optimal experiment with nonlinear constraints	58
5.7	Real and simulated blood glucose level	59

List of Tables

4.1	Overall sensitivity for healthy and diabetic type 1 person	41
4.2	Correlation matrix for a healthy person	42
4.3	Correlation matrix for a diabetic person	42
4.4	Parameter vector of size 3 for healthy person	44
4.5	Parameter vector of size 3 for diabetic person	44
4.6	Parameter vector of size 6 for healthy person	45
4.7	Parameter vector of size 6 for diabtic person	45
4.8	Overview of parameter vector with lowest optimality criterion for healthy person	45
4.9	Overview of rank for a healthy person	46
5.1	Overall sensitivity of parameters	52
5.2	RDE results	53
1	Parameter values form the litteraturel	67
2	Model parameter description for the minimal model	68

Project overview

1

1.1 Diabetes

Energy is a necessity for all living organisms. Thus, for a human to be able to perform daily activities, the body has a certain need of energy. The energy comes from food and drink in the form of carbohydrates, protein and fat. The body can not make use of carbohydrates, protein and fat directly. Hence, almost all food needs to be converted into a simple sugar called glucose. Glucose is absorbed by the bloodstream, where its level is regulated by insulin - to be stored, produced, or broken down and used to form ATP, which in turn powers every activity in the cell. Insulin keeps the blood glucose level in a certain range, and is therefore very important in the glucose metabolism.

A person diagnosed with type 1 diabetes mellitus do not produce insulin, which means that no insulin is present to regulate the blood glucose level. The same problem occurs for a person diagnosed with type 2 diabetes mellitus, where the insulin production is insufficient in combination with insulin resistance. Because no, or too small, amounts of insulin is present to store and distribute blood glucose, both types may suffer from high glucose blood levels, known as hyperglycemia. Long-term hyperglycemia may have serious consequences, which include heart disease, strokes and kidney failure and diabetic reinopathy where eyesight is affected, which in turn may result in blindness. In addition, it may results in poor circulation of limbs, which may lead to amputations. There is also a risk for hypoglycemia, which is when the blood glucose level is too low. Because the brain almost exclusively use glucose as energy source, a blood sugar too low may not meet the brains glucose requirements. Hence, diabetic hyperglycemia may cause effects on the function of the brain. This effects may have the form of unconsciousness or diabetic coma. In some rare cases, hypoglycemia even cause permanent brain damage and death. To avoid this, the diabetic person needs to inject exogenous insulin into the body in order to keep the glucose level in the target range.

The exact reason for both type 1 and type 2 diabetes mellitus are not completely understood. Type 1 diabetes mellitus is most likely due to genetic predisposition, whereas type 2 diabetes mellitus seem to depend highly on environmental factors. Excess caloric intake, inactivity and obesity all seem to play a part in the pathogenesis of type 2 diabetes mellitus. Today, over 340 million people are diagnosed with diabetes, and type 2 diabetes mellitus comprises 90% of these people. Because of social changes, obesity and overweight has more than double since 1980 [25], and since

this trend most likely will continue, diabetes is projected to increase by over 80% in upper-middle-income countries [24].

The critical part being diagnosed with diabetes, is the insulin administration. Each year about 3.2 million diabetes-related deaths worldwide are reported annually [20], and this number is assumed underestimated. In addition, diabetes may cause blindness, kidney failure and more than 60% of nontraumatic lower-limb amputations occur in people with diabetes [1]. Hence, diabetes may lead to various negative consequences for the diabetic person, which in turn cause enormous national health costs. This emphasizes the importance of insulin administration, and to be able to decrease the personal and national side effects of diabetes, more reliable insulin administration methods are needed.

1.2 Insulin administration

Different types of devices are available to help persons with diabetes to manage their disease. Today, the most common method is self-monitoring of blood glucose (SMBG), where insulin is injected directly into the fat tissue. In that case, a specific insulin dose is injected by a syringe or an insulin pen. A syringe is the simplest device, and need to be filled with insulin solution before it can be injected into the body. Insulin pens, on the other hand, automatically release the pre-selected quantity of insulin when pushed into the body, and is able to store insulin using cartridges. During the day, there is also a need of checking glucose levels to see if the insulin dose is able to keep the glucose level in the target range. This is done by a blood glucose meter, where a small drop of blood, obtained by pricking the skin with a lancet, is placed on a strip. Afterwards, the strip is placed in the meter, and the blood glucose level is calculated. These measurements are often logged, to check if the given insulin dose is able to keep the blood glucose levels within the range.

For both diabetes type 1 and type 2, the time course of insulin action requires three or more injections per day. Because of the expected increase in blood glucose during a meal, the injection is often set 15-30 minutes before a meal. The time for when the injection is set, mainly depends on the type of insulin. In addition, the blood glucose needs to be measured - for a type 1 diabetic as much as 4-6 times a day. The timing, the type and amount of insulin, is individual and is somewhat decided by a doctor. However, the amount of needed insulin depends on the daily activities, which means that a diabetic must be able to calculate the insulin dose according to the given guidelines. Some factors which may affect the needed dose of insulin are:

- Type of food
- Amount of food
- Number of meals
- Physical activities

Imagine a meal, which is often a composition of carbohydrates, protein and fat. Carbohydrates enter the bloodstream quite fast - in contradiction to proteins and fat, which take about four to eight hours to show up in the bloodstream. Even though the amount of protein and fat will affect the blood glucose, the amount of needed

insulin depends mostly on carbohydrate intake. Therefore carbohydrate counting is important for a diabetic. However, different kind of carbohydrates, have different effect on the glucose levels. Sweets, fruits and mashed potato are examples of rapid-acting carbohydrate, which will cause high glucose spikes. On the other side, beans and nuts are examples of slow-acting carbohydrate, and the glucose will be absorbed slowly into the bloodstream. Hence, counting carbohydrates is not an easy task. If a meal contained mostly slow-acting carbohydrate and insulin is injected to match the amount of carbohydrate, the insulin may work too quickly. This could make the blood glucose levels fall before the carbohydrate is absorbed, which could result in blood glucose levels both below and over the target range. Hence, the type of food is important, but also the amount of food. If the food portion is bigger than normal, more insulin is also needed - and conversely. The number of meals during a day needs also to be taken into consideration. If a meal is skipped, this may lead to low glucose levels and cause hypoglycemia. Exercise and physical activities increase glucose utilization, which is also an important factor. Because of the natural reduction of glucose in the blood stream during physical activities, less insulin is needed. If a insulin dose too big is set before expected or unexpected exercise, this might result in hypoglycemia. On the other hand, if an expected exercise is skipped, this may result in hyperglycemia because of lack of insulin. Other factors that may affect blood glucose level is certain types of illnesses and effect of other medical medicines.

As stated above, knowing how much insulin, and when the injection should take place, is not easy. The blood-glucose meter gives an indication of the current glucose level and may work as a long-term guide for the needed amount of insulin. However, hyperglycemia may occur in long periods between glucose measurements, and glucose levels may change rapidly after a measurement. Because of this current issues regarding insulin administration, and the economic potential due to the huge diabetes care device market, companies are competing to develop new methods for insulin administration. The goal is automatic control of the blood glucose level, where feedback of real-time blood glucose data is connected to an insulin pump, which reads the glucose level and dispense the precise amount of insulin needed. Hence, continuous glucose monitoring plays an important role in order to improve insulin administration, and give the diabetic an easier life.

1.3 Continious glucose monitoring

Even though self-monitoring of blood glucose has been used since the first blood glucose meter was introduced in 1970, current methods for glucose monitoring is not ideal. The finger-pricking, which is the most common method, has several disadvantages; the method is not painless, and many people dislike seeing blood and using sharp objects. In addition, there is a risk of infection, and over long term this practice can result in damage of the finger tissue. Because this method involves blood, and taking the size of the glucose meter into consideration, glucose measurements need to be planned, and is not practical for continuous monitoring of blood glucose.

Because of the problems regarding conventional glucose monitoring, and because of the development of insulin pumps, other blood glucose meters have been developed. The new devices focus on continuous measurements with a glucose sensor inserted into the abdomen. Further, the sensor takes reading and reports to a moni-

tor. After two or three days, the sensor is removed and replaced with a new sensor. In this way, the diabetic is able to check the glucose level during the day, and on some devices an alarm is triggered if hyperglycemia or hypoglycemia occur. However, the monitor needs to be calibrated several times a day. This is done by the person inputting the results from conventional finger sticks, which means that this method do not necessary reduce the number of needed finger sticks. There has also been problems regarding the reliability of the measurements; drifting and/or diminishing of the sensor signal has been reported due to the formation of proteins and other biological matter on the sensor surface.



Figure 1.1: Continious blood glucose sensor with insulin pump

The glucose monitoring methods that have been mentioned so far, have been invasive. To avoid the consequences regarding finger-pricking, and to be able to continuous monitor the glucose level, it is clearly desirable with noninvasive glucose measurements. Different methods for non-invasive glucose measurements are under study, and an overview is given by So et al.(2012)[5]. Some of these methods are based on ultrasound technology or different types of spectroscopy, where near infrared spectroscopy (NIR) has become a promising technology, among others [5]. NIR is a spectroscopic method which uses the near-infrared region of the electromagnetic spectrum, where the measurements of the absorption of NIR-beams are used to characterize the tissue. This in turn can be used to calculate the level of glucose in the subcutaneous tissue.

Regarding noninvasive technologies, many research groups have explored the wide variety of approaches, and tried to develop a non-invasive blood glucose measurement device that can provide stable and reliable results. Unfortunately, none of these technologies have produced a commercially available, clinically reliable device [5]. Because of the huge market for a successful, noninvasive glucose monitor, there is a race for research teams to develop a precise and accurate equipment.

1.4 Aim of the project

The aim of the project is to study a mathematical model of the glucose metabolism, which is supposed to be used in order to develop a non-invasive glucose measurement device. This device is supposed to estimate and predict blood glucose level in both healthy persons, and persons with diabetes. With the combination of non-invasive measurements from NIR and dielectric spectroscopy, this measurements is

processed and used in a Kalman filter with the glucose metabolism model. It is assumed that this will make it possible to estimate the glucose level in real-time. The project is in cooperation with Prediktor AS, where the noninvasive glucose measurement device currently is under development.

In more detail, this project will contain the following:

1. Study existing mathematical models regarding glucose metabolism in the literature, and choose a model which fits the requirements
2. Discuss different measurements that may be needed for calibration and real-time updates for the model
3. Analyze the model with regard to parameter identifiability

Literature study

2

2.1 Introduction

A dynamic model describing the glucose metabolism in order to control glucose level, has been studied for decades. It began with simple models of the insulin-glucose system - also known as minimal models, and later progressed to large-scale simulation models, known as maximal models. Minimal models is one class of models, which are based on the concept that the dynamics of the biological system should be described by a minimum number of identifiable parameters [8]. Therefore, the model only describes the main characteristics of the system. The basis for the minimal model is the information content in a glucose test, where blood glucose and insulin samples of a fasting person are collected after a meal, where the information is used for parameter identification. Because the minimal model strategy has been, and still is, very successful [8], the minimal model has been widely employed by more than one thousand papers. Maximal models, on the other hand, are comprehensive descriptions, which consolidate large amount of biological knowledge. These models are often nonlinear with a high order, and with a large number of parameters. Hence, maximal models are generally not identifiable without massive experimental investigation. These models are often used for simulation, and have made it possible to perform simulation trials in replacement of animal testing.

One may wonder why there is such a large number of different mathematical models describing the glucose metabolism. This is partly because some issues regarding the glucose metabolism are not completely understood. Also, in the model, it is not possible to include every single process which affects the glucose metabolism. Therefore, the models are often based on different theories regarding the glucose metabolism; therefore, in some models a specific process may be modeled, while the same process is ignored in another model. In this chapter we will take a look at some models which might be relevant according to this project. These are models that describe some of following properties

- The general glucose-insulin dynamic in both healthy, and persons with diabetes
- How exercise affect the blood glucose level
- Insulin secretion in healthy persons

In order to understand the concepts behind the glucose metabolism models, a short review describing the glucose metabolism is given in the following section.

2.2 Theory

2.2.1 Glucose metabolism in a healthy person

The level of plasma glucose concentration depends on the in- and outflow within the bloodstream. The inflow depends on the food intake and the glucose production from liver. The outflow depends on the glucose utilization by the muscle and skeleton cells, and the brain cells. The utilization in muscle and skeleton cells depends highly on the level of physical activity, while the cells in the brain is assumed to be rather constant. The outflow is also affected by the rate at which glucose is stored in the liver, and the clearance of glucose through urine. The glucose utilization in muscle and skeleton cells, and the liver production and storing process, are mainly controlled by insulin to keep the glucose level within the range of 70-150 [mg/dl]. This can be shown in figure 2.1, which illustrates the main processes affecting the blood glucose level. Dashed lines indicate the flows which is insulin dependent, while solid line represent insulin independent flows.

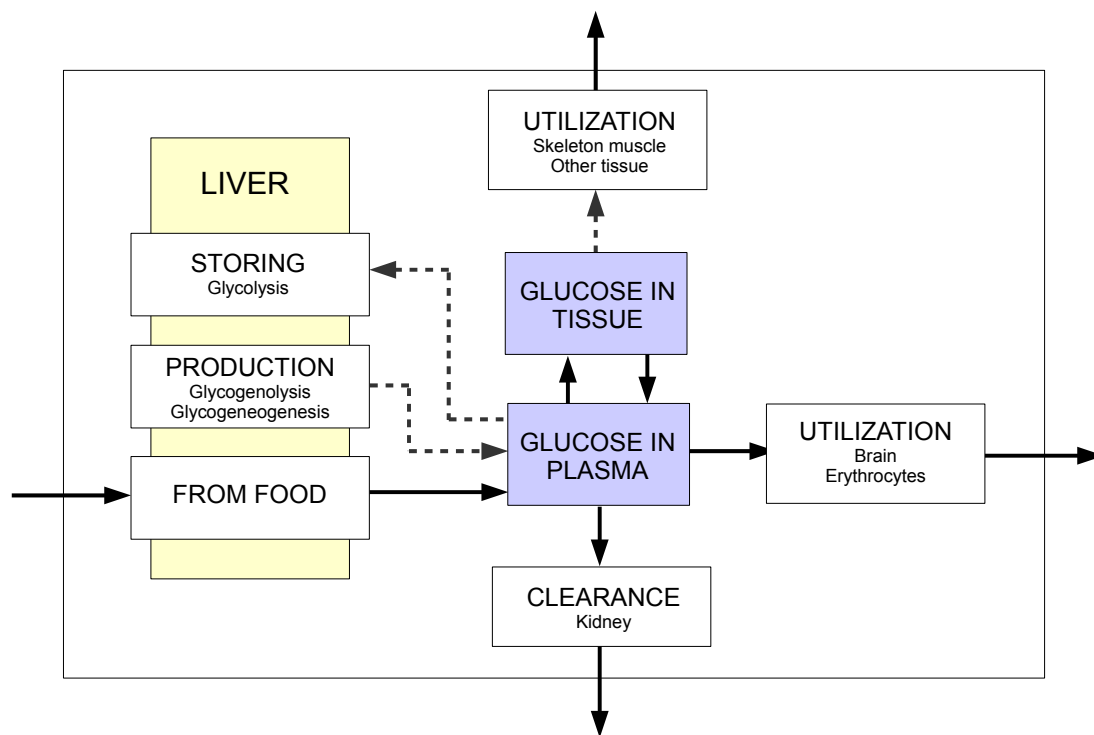


Figure 2.1: Glucose metabolism process

Insulin and glucagon are two hormones secreted from the islets of Langerhans in the pancreas. Glucagon is secreted from the α -cells when the blood glucose level needs to be increased. Glucagon triggers glycogenolysis, which is a process where stored glycogen in the liver is broken down to glucose and released into the bloodstream. When the storage of glycogen is empty, glucagon triggers gluconeogenesis, where glucose is generated from non-carbohydrate and released into the bloodstream. Insulin is secreted in pulses by the β -cells in the pancreas. This is a complex process,

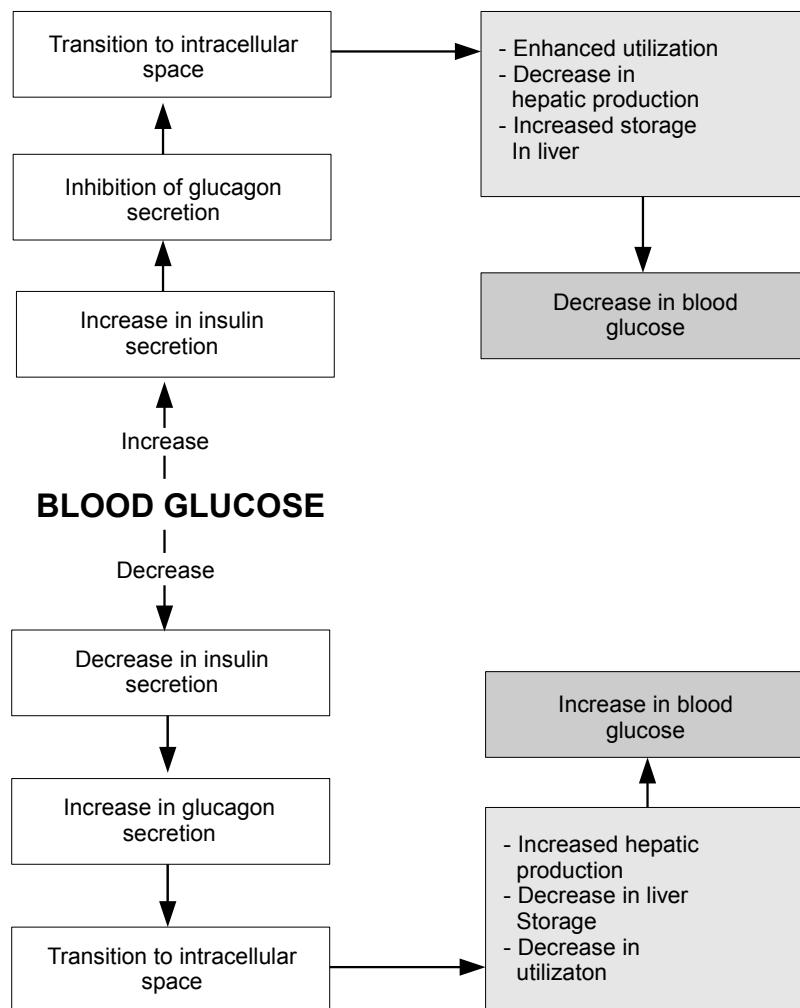


Figure 2.2: Insulin control

and the secretion process is not completely understood. Insulin is secreted in order to keep the glucose level in the target range, and works as described in the following

- Insulin enhance the insulin dependent glucose utilization. Insulin binds to the receptor of skeleton muscle cells. This activates the glucose transporter GLUT4 inside the cell, which in turn transport glucose from the membrane and into the cell to form ATP. How much the insulin enhance these utilization is not completely known.
- If the cells have sufficient supplies of ATP, insulin triggers glycogenesis, which is a process transforming glucose into glycogen in the liver, where it is stored.
- Insulin inhibits the secretion of glucagon [29], and therefore indirectly controls glycogenolysis and gluconeogenes.

How sensitive the body is to the effect of insulin - in other words; the decrease in glucose plasma due to a certain amount of insulin, is described by the insulin sensitiv-

ity, which varies among individuals. The sensitivity depends on the level of physical activity, which has proven[18] to increase the insulin sensitivity both during exercise and a certain time afterwards. How insulin controls the glucose level is illustrated in figure 2.2. As can be seen, insulin do not affect glucose level directly, but through remote insulin, which is the insulin in the intracellular space which directly affects the glucose utilization and storing. The processes described do not happen immediately, but are a delayed response which occur after several biochemical processes triggered by the two hormones.

2.2.2 Glucose metabolism in a diabetic

In type 1 diabetes, the islets of Langerhans are destroyed by the immune system, which makes the number and size of the islets eventually reduced. Therefore, the secretion of insulin by the β -cells are almost nonexistent. In type 2 diabetes, the islet cells are decreased and cannot produce sufficient amounts of properly-functioning insulin. In addition, the cells within the muscles, liver and fat tissue do not respond normally to the insulin level. In both cases, there are not enough insulin present which means that processes go forth at high rates, completely unregulated. Hepatic glucose production will not be inhibited, and there are no insulin to enhance the glucose utilization. This may cause the diabetic to suffer of constant hyperglycemia.

2.3 Minimal model approach

The minimal model was published by Bergman, and consists of three equations describing plasma glucose concentration $G(t)$, plasma insulin concentration $I(t)$ and remote insulin $X(t)$. This is shown in equations 2.1, 2.2 and 2.3. The model describes glucose utilization and hepatic production, which is both insulin-dependent and insulin-independent. $U(t)$ is the plasma insulin appearance rate, and $D(t)$ describes the exogenous glucose input.

$$\frac{dG}{dt} = -p_1G(t) - X(t)G(t) + p_1G_b + D(t) \quad (2.1)$$

$$\frac{dX}{dt} = -p_2X(t) + p_3[(I(t) - I_b)] \quad (2.2)$$

$$\frac{dI}{dt} = -nI(t) + p_4 \frac{U(t)}{V_I} \quad (2.3)$$

This model assumes that glucose and insulin are intravenous injected into the bloodstream. If this is the case, the model is proven to be a priori uniquely identifiable. Because intravenous injections are not the case for neither healthy persons or persons with diabetes, the model have been both modified and extended in order to describe the glucose metabolism when insulin is injected in the subcutaneous layer. If a Bergman model is chosen to describe the glucose-insulin dynamic, the following needs to be added to the model:

- Description of how an oral glucose intake is being absorbed into the bloodstream
- Description of the pancreatic β -cell production
- Description of how an injection of insulin in the subcutaneous layer appears into the bloodstream
- How physical activity affect blood glucose

2.3.1 Oral glucose intake

A model is needed to describe how an oral food intake appears into the bloodstream. This is usually done by a model describing how a meal carbohydrate load $D_g(t)$ is processed through the digestive system. There is some differences in the complexity of the models. Some models describe the process as a two-compartment model representing a certain delay, while some models are more physiological correct and describes the rate of glucose absorption via the gut wall according to the rate of gastric emptying.

2.3.2 Pancreatic production

For a healthy person, the insulin which controls the blood glucose, is secreted by the pancreatic β -cells in the portal vein. Some diabetic also produce a certain amount of insulin. In this case, $U(t)$ in equation 2.3 needs to be modeled to describe secreted insulin, which is described in different ways in the literature. In the work of Sturis et al. (2000) [21], the pancreatic production is a function depending on the plasma glucose level. The pancreatic production has also been described by a two-compartment model depending on both the glucose level and its rate of change.

2.3.3 Effect of physical activity

The minimal model needs to describe the physiological changes due to physical activity. During, and a certain period after exercise, the insulin sensitivity is increased, which seems to be because of insulin-dependent augmented availability of GLUT4. In the model by Breton et al. (2008) [2], the increased insulin sensitivity is due to increased insulin action described by a parameter Z , which depends on the measured heart rate. Another exercise model by Parker et al. (2007) [27], is more complex. This model uses the percentage PVO_2^{max} of the maximal oxygen consumption VO_2^{max} as an input to the model in order to quantify exercise intensity. In addition to augmented availability of GLUT4, this model describes the following

- The increase in glucose uptake due to increasing exercise intensity
- The increase in hepatic glucose release due to increasing exercise intensity
- The decrease in glucose production from glycogenolysis because of limited supply of glycogen in the liver
- The removal of insulin in the circulatory system due to physiological changes

The added effect of physical activity is seen in more recent years, and not many models which describes this effect are found in the literature.

2.3.4 Subcutaneous insulin injection

Because insulin is not injected directly into the bloodstream, there is a need to incorporate the subcutaneous insulin kinetics into the model, which applies to both diabetic type 1 and type 2 patients. The major difficulties in modeling include accounting for the distribution in the subcutaneous depot and transport to plasma [16]. The time between the injection of insulin and its appearances in the plasma takes about 30 min to 1 hour. Many factors, such as the injected volume of insulin, the depth of the injection, and changes of blood flow around the injection site, affects the insulin absorption. In addition, the absorption rate of subcutaneously injected insulin decreases with increasing insulin concentrations and increasing volumes. The quantitative description of insulin absorption is thus a difficult task, and everything from simple one-compartment models, to nonlinear partial differential equations, have been developed to describe the process.

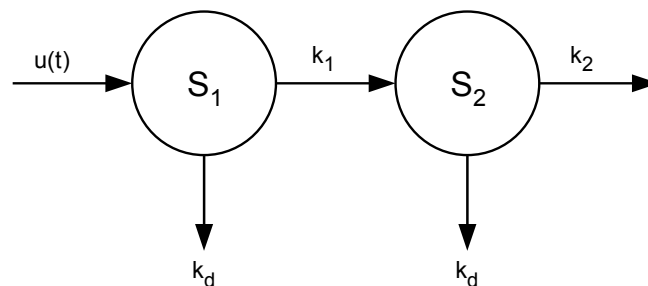


Figure 2.3: Example of subcutaneous insulin kinetics

For minimal models, a one- or a two-compartment is often used to describe the subcutaneous insulin kinetics. A two-compartment model is shown in figure 2.3. In this model $u(t)$ is the injected insulin in the subcutaneous layer, and k_d is the degradation rate. The rate of appearance in insulin plasma equals $U(t) = \frac{k_2}{V_d}$, where V_d is the distribution volume of insulin. Other models are various forms of the one shown in figure 2.3. Some models may have a degradation rate in the second compartment or no degradation rate at all, and in some cases the flow rate k_1 equals the flow rate k_2 .

2.4 Maximal model approach

Different maximal models have been developed to describe the glucose-insulin interaction. These models are often complex, and describe all processes which affects the glucose level.

2.4.1 Meal simulation model

The simulation model in Cobelli et al. (2007) [7] describes the glucose-insulin system in the postprandial state, which focus on quantitative physiological events after a meal. The model consists of a glucose and insulin subsystem. The glucose subsystem is described by a two-compartment model, one representing glucose mass in plasma and rapidly equilibrating tissues, $G_p(t)$. The other represents glucose in slowly equilibrating tissues, $G_t(t)$. The insulin subsystem is also represented by a two-compartment model, which describes the insulin masses in liver, $I_l(t)$ and in plasma, $I_p(t)$. The simulation model has been extended and modified to also include the effect of physical activity.

The glucose subsystem is shown in equation 2.4. Both G_p and G_t depends on a number of submodels describing the various unit processes. $EGP(t)$ is the endogenous glucose production, $R_a(t)$ is the rate of appearance of glucose from food, $E(t)$ is the renal extraction, and $U_{id}(t)$ and U_{ii} are insulin-dependent and insulin-independent utilization.

$$\begin{cases} \dot{G}_p(t) = EGP(t) + Ra(t) - U_{ii}(t) - E(t) - k_1 \cdot G_p(t) + k_2 \cdot G_t(t) \\ \dot{G}_t(t) = -U_{id}(t) + k_1 \cdot G_p(t) - k_2 \cdot G_t(t) \\ G(t) = \frac{G_p}{V_g} \end{cases} \quad (2.4)$$

The insulin submodel is shown in equation 2.5, where I_l is the insulin in liver and I_p is insulin in plasma. As can be seen, additional submodels is also necessary to describe the different processes, where $S(t)$ is the insulin secreted into the portal vein.

$$\begin{cases} \dot{I}_l(t) = -(m_1 + m_3(t)) \cdot I_l(t) + m_2 I_p(t) + S(t) \\ \dot{I}_p(t) = -(m_2 + m_4) \cdot I_p(t) + m_1 \cdot I_l(t) \\ I(t) = \frac{I_p}{V_I} \end{cases} \quad (2.5)$$

2.4.2 Model at molecular level

In Liu et al. (2008) [32], a mathematical model is made at the molecular level. Because of cross talk and feedback among metabolic pathways and signaling, it was stated that more details of the system could be included at the molecular level. The following processes are considered

- The concentration of insulin and glucagon in plasma, and the transition process time delay for insulin and glucagon in plasma to enter the cellular space.
- The dynamics between intracellular and receptor-bounded insulin and glucagon.
- The concentration of glycogen and plasma glucose, which depends on the concentration of receptor-bounded insulin and glucagon.

2.4.3 Oscillatory insulin secretion

Experiments have revealed that the release of insulin from the pancreas occurs in an oscillatory fashion with a typical period of 80-150 min [21]. These slow oscillations is mainly in the portal vein, and they are assumed to have a important influence on several hepatic processes. The underlying mechanisms for the oscillations is most likely a result from an instability in the insulin-glucose feedback system. Because experiments have shown that a pulsating supply of insulin can have a higher hypoglycemic effect than a constant supply, models describing this phenomenon have been of interest.

Sturis et al.(2000) [21] suggested the model viewed in equations 2.6, 2.7 and 2.8 for the description of slow oscillations. The model has three main variables; plasma insulin I_p , intracellular insulin I_i and plasma glucose G . The purpose of both I_p and I_i is to represent the delay between insulin action and plasma insulin. $f_5(x_3)$ is a function describing the hepatic glucose production, which is a delayed response to the insulin level represented by x_3 . The delay is described by a third order model, and is actually a part of the model. Insulin secretion, rate of appearance of glucose and glucose utilization, is described by different functions.

$$\frac{dI_p}{dt} = f_1(G) - E \left(\frac{I_p}{V_p} - \frac{I_i}{V_i} \right) - \frac{I_p}{t_p} \quad (2.6)$$

$$\frac{dI_i}{dt} = E \left(\frac{I_p}{V_p} - \frac{I_i}{V_i} \right) - \frac{I_i}{t_i} \quad (2.7)$$

$$\frac{dG}{dt} = G_{in} - f_2(G) - f_3(G)f_4(I_i) + f_5(x_3) \quad (2.8)$$

The function $f_1(G)$ describes the pancreatic insulin production and is controlled by the glucose concentration. The function $f_2(G)$ is the insulin-independent glucose utilization, and $f_3(G)$ describes the glucose utilization by muscle and fat cells.

Instead of a third order model representing the delay, similar models have been represented by delay differential equations in order to represent the delay between plasma and intracellular insulin, and the delayed response according to the hepatic production.

2.5 Parameter identification techniques

Various methods have been used to identify the parameters in glucose metabolism describing models, where the complexity of the identification method often depends on the complexity of the model. For the simple minimal model, intravenous glucose tolerance tests (IVGTT) have been used to identify the parameters. In an IVGTT, glucose is intravenously injected, and then both glucose blood level and insulin level are measured with blood samples. Using the injected glucose input, and insulin and glucose output data, it is possible to identify the parameters.

More complex models, such as maximal models, are using other methods for estimating the parameters. A common method is to use tracer studies. Tracers, which

is some chemical composition, is given in the food or injected into the bloodstream and tissue. Technology such as positron emission tomography or nuclear magnetic resonance, are able to detect the tracers inside the body. This have made it possible to calculate such as the rate of glucose appearance, glucose and insulin fluxes, glucose utilization and insulin secretion. In this way, the parameters for the different sub-models have been found. The tracer experiments have usually been done on several people, and then the mean value is used for the final model.

Glucose metabolism model

3

3.1 Choice of model

In chapter 2, a short literature review described different ways to model the glucose metabolism. For our purposes, it is desirable that the model predicts the glucose level at some accuracy and is suited for real-time estimation. Because biochemical processes affecting the glucose metabolism are assumed to be highly individual, it seems to be a need for calibrating the glucose metabolism model to each specific person. The glucose metabolism is normally described by a maximal model, or an extended and modified minimal model. Because of the complexity, the model parameters of maximal models need enormous amounts of testing to be identified, and can only be identified by tracer tests. Such complex test techniques are not supposed to be performed for this project, which means that calibrating can not be performed for a maximal model. In various tests done by Prediktor [17], the model developed by Cobelli et al. (2007)[7] did not give a satisfactory result. On the other hand, a modified and extended minimal model showed the ability to estimate the blood glucose level, where the minimal model was implemented in a Kalman filter together with measurements of blood glucose values. This model is shown in the following, and is the foundation for the future work.

In equations 3.1 and 3.2, the minimal model is shown. This model is found in Bergman et al. (1979)[26], and is extended to also include the plasma insulin concentration I . As stated in section 2.3, there is a need to define $D(t)$ to describe the oral glucose intake, and to define $U(t)$ to describe the subcutaneous insulin injection. In addition, the model does not describe the pancreatic insulin secretion which also needs to be added.

$$\frac{dG}{dt} = -p_1G(t) - X(t)G(t) + p_1G_b + D(t) \quad (3.1)$$

$$\frac{dX}{dt} = -p_2X(t) + p_3[(I(t) - I_b)] \quad (3.2)$$

$$\frac{dI}{dt} = -nI(t) + p_4 \frac{U(t)}{V_I} \quad (3.3)$$

Oral glucose intake

In order to describe the appearance of glucose $D(t)$ in the blood after a carbohydrate intake, a submodel describing the glucose through the stomach and gut was added. The submodel is taken from Cobelli et al. (2007) [8], which is given as

$$\frac{Q_{sto}}{dt} = Q_{sto1} + Q_{sto2} \quad (3.4)$$

$$\frac{Q_{sto1}}{dt} = -k_{gri}Q_{sto1} + Dd(t) \quad (3.5)$$

$$\frac{Q_{sto2}}{dt} = -k_{emp}(Q_{sto})Q_{sto2} + k_{gri}Q_{sto1} \quad (3.6)$$

$$\frac{Q_{gut}}{dt} = -k_{abs}Q_{gut} + k_{emp}(Q_{sto})Q_{sto2} \quad (3.7)$$

where rate of appearance of glucose into the bloodstream is given as

$$R_a = \frac{fk_{abs}Q_{gut}}{BW} \quad (3.8)$$

All parameters are constants, except from k_{emp} which is the rate of gastric emptying. The gastric emptying depends nonlinearly on the size of the meal and the amount of nutrient in the stomach, and is given by the following function

$$k_{emp} = k_{min} + \frac{k_{max} - k_{min}}{2} \cdot \{ \tanh[\alpha(Q_{sto} - b \cdot u_{meal})] - \tanh[\beta(Q_{sto} - C \cdot u_{meal}) + 2] \} \quad (3.9)$$

Four differential equations and the function describing k_{empt} really increases the complexity of the model. Therefore, this submodel was simplified to a two-compartment model

$$\frac{dQ_{sto}}{dt} = -k_{emp}Q_{sto} + u_{meal} \quad (3.10)$$

$$\frac{dQ_{gut}}{dt} = -k_{abs}Q_{gut} + k_{emp}Q_{sto} \quad (3.11)$$

$$R_a = fk_{abs}Q_{gut} \quad (3.12)$$

The glucose intake is the input u_{meal} , while k_{abs} is the rate of intestinal absorption.

The rate of appearance is described by R_a , and the parameter f is the fraction of intestinal glucose absorption which appears in plasma. Because of the simplification of the model, the function describing k_{empt} cannot be used. It is assumed that this parameter will be defined as a constant. The oral glucose intake is found as

$$D(t) = R_a/V_p \quad (3.13)$$

Carbohydrate-containing food can actually be classified by the concept called glycemic index (GI). The GI compares the suddenly increase in in the plasma glucose concentration from a fixed amount of available carbohydrate in a test food, with the glycemic response excited from the same amount of carbohydrate in a standardized reference food [28]. Carbohydrates affect the blood glucose differently depending on the GI, where carbohydrates with high GI result in an earlier rise in the blood glucose level. The glucose model does not take this into consideration, and does only take the amount of carbohydrate as input.

Subcutaneous insulin injection

Because insulin is assumed intravenously injected in the original minimal model, the minimal model need to be extended to the describe the subcutaneous insulin injection. This is done by describing the insulin injection as a two-compartment model as described in equation 3.14 and 3.15. This is a quite simple model, with no degradation rate and with equal time constants. The injection u_{ins} takes place in S_1 , and insulin enters the bloodstream in plasma insulin through the second compartment S_2 .

$$\frac{dS_1}{dt} = -\frac{1}{T_d}S_1 + u_{ins} \quad (3.14)$$

$$\frac{dS_2}{dt} = \frac{1}{T_d}(S_1 - S_2) \quad (3.15)$$

Now, the insulin injected insulin $U(t)$ from equation 3.8 can represented as $U(t) = S_2$. Setting parameter $p_4 = 1/T_d$, the plasma insulin concentration can be written as

$$\frac{dI}{dt} = nI(t) + \frac{1}{V_I T_d}S_2 \quad (3.16)$$

The input u_{ins} represents both the constant basal insulin u_b and the bolus insulin u_l . The basal insulin is the insulin which is always present, and is independent from glucose intake. For a diabetic person, u_l is the needed injected insulin depending on the carbohydrate intake. Therefore, u_{ins} is given as

$$u_{ins} = u_b + u_l \quad (3.17)$$

where

$$u_b = nV_I I_b \quad (3.18)$$

Even though the basal insulin is missing for a diabetic type 1 person, it is assumed that the injected long-acting insulin approximates the basal insulin u_b . Further, the rapid-acting injected insulin which is needed before meals, is represented by the term u_l . For a healthy, there is no injected insulin, which means that the input is given as $u_{ins} = u_b$. Hence, the input u_{ins} represents a healthy person as well as a diabetic person.

Pancreatic insulin production

For a healthy person, the input u_{ins} represents the constant basal insulin. In addition, we also need to add the pancreatic insulin secretion in equation 3.16, which cause the rise of insulin after a carbohydrate intake. To describe the insulin secretion in a healthy person, a function from Sturis et al.(2000)[21] was chosen. The function is shown in equation 3.19, where R_m represents the maximal rate of insulin production, C_1 is the parameter which decides when insulin is secreted, while a_1 in simple term decides how much insulin is secreted. In type 1 diabetes patients, $f_G(G)$ is set to zero.

$$f_G(G) = \frac{R_m}{1 + \exp((C_1 - G)/a_1)} \quad (3.19)$$

Exercise

The glucose metabolism model also need to account for the effect of exercise. The chosen exercise model is shown in equations 3.20, 3.21 and 3.22, and is a modified form of the exercise model by Breton et al.(2008) [2]. The model describes the changes in insulin sensitivity and insulin-independent glucose uptake due to physical activity. The increase in insulin sensitivity is described by insulin action Z , which represents the increased insulin-dependent glucose utilization. Z depends on the measured heart rate HR , and decreases slowly after HR equals the basal heart rate HR_b . This is according to the assumed increase in insulin sensitivity, which occurs after exercise.

$$\frac{dZ}{dt} = - \left(f(Y) + \frac{1}{T_{ex}} \right) \cdot Z + f(Y) \quad (3.20)$$

$$Y = \frac{HR}{HR_b} - 1 \quad (3.21)$$

$$f(Y) = \frac{aY^{nE}}{1 + aY^{nE}} \quad (3.22)$$

In practice, this means that two terms need to be added in the plasma glucose differential equation \dot{G} . The term αZXG which described the increased insulin dependent glucose utilization, and the term βYG which describes the insulin independent glucose utilization due to physical activity.

Final model

When adding the description of oral glucose intake, pancreatic insulin secretion, subcutaneous insulin injection and effects of physical activity, the minimal model take the following form

$$\frac{dG}{dt} = -(p_1 + (1 + \alpha Z)X)G + p_1 G_b - \beta Y G + \frac{R_a}{V_p} \quad (3.23)$$

$$\frac{dX}{dt} = -p_2 X(t) + p_3 [(I(t) - I_b)] \quad (3.24)$$

$$\frac{dI}{dt} = -nI(t) + \frac{1}{V_I T_d} S_2 + f_G(G) \quad (3.25)$$

Because the insulin dynamic is assumed fast, the equation describing plasma insulin in equation 3.25 is reduced and shown in equation 3.26. In some cases the diabetic person is able to some extent, produce small amounts of insulin. Therefore, the term I_{add} which describes unmodeled insulin generation, was added.

$$I = \frac{1}{n} \left[\frac{1}{V_I T_d} S_2 + \frac{R_m}{1 + \exp((C_1 - G)/a_1)} + I_{add} \right] \quad (3.26)$$

where

$$\frac{dI_{add}}{dt} = 0 \quad (3.27)$$

Hence, the glucose model is described by equation 3.23, 3.24, 3.26 and 3.27. In addition to the gut model in equations 3.10 and 3.11, the subcutaneous insulin submodel in 3.14 and 3.15, the pancreatic insulin secretion function 3.19 and the exercise model given in equation 3.20 to 3.22. All parameters are shown in table 2 in the appendix.

The additional submodels increased the complexity of the original minimal model. The final model represents a nonlinear system which consists of 8 differential equations, where the state vector x is given as

$$x = [G \quad X \quad S_1 \quad S_2 \quad Q_{sto} \quad Q_{gut} \quad Z \quad I_{add}] \quad (3.28)$$

and input vector

$$u = [u_{meal} \quad u_{ins} \quad Y] \quad (3.29)$$

The model will take different form depending on whether it is supposed to describe a healthy or a diabetic type 1 person. However, the only difference is the pancreatic insulin secretion function $f_G(G)$, which for a diabetic person is set to zero.

3.2 Simulation of the glucose model

Simulation plays an important part in order to check the qualitative behavior of a system. In our case, the simulation of the glucose metabolism model involves the numerical solution of the differential equations presented in the previous section. Different types of numerical integrators can be applied in order to solve the differential equations. Every method has its own properties, and which method to use depends on the system to be simulated. The numerical solution is approximated at each time step h which needs to be defined. If the time step is set too high, the error in each iteration may be very high which results in a poor simulation. In some cases the accumulated error in each time step is so big, that it results in an unstable system. Therefore, the choice of time step h is important.

Different simulation tool exists, but in this project only Matlab will be used. In the case of solving the differential equations, we can either implement a numerical scheme on our own or use one of the Matlab built-in differential equation solvers. The advantage of the Matlab differential equation solvers is that we don't need to specify the time step. The solver is able to choose a step size which meets a specified error tolerance. The solvers will vary the step size in order to produce a solution which is accurate to the given error. Even though implementing a numerical scheme on our own would reduce the computational cost, the model was simulated with the Matlab built in differential equations solver *ode45*, which is based on an explicit Runge-Kutta method. At each iteration, the function calculates the numerical solution to the initial value problem. The parameters in the model are taken from the literature and can be found in the appendix.

3.2.1 Simulation for a healthy person

When the equations describing the glucose model from the previous chapter is organized, and functions are inserted into the differential equations, we get the following system:

$$f(x_k, u_k) = \begin{bmatrix} -(p_1 + (1 + \alpha_e Z)X)G + p_1 G_b - \beta_e YG + \frac{f k_{abs} Q_{gut}}{V_p} \\ -p_2 X + p_3 \left(\frac{T_i}{V_i} \left(\frac{S_2}{T_d} + \frac{R_m}{1 + \exp((C_1 - G)/a_1)} \right) - I_b + I_{add} \right) \\ -\frac{1}{T_d} S_1 + u_{ins} \\ \frac{1}{T_d} (S_1 - S_2) \\ -k_{emp} Q_{sto} + u_{meal} \\ -k_{abs} Q_{gut} + k_{emp} Q_{sto} \\ -\left(f(Y) + \frac{1}{T_{ex}} \right) \cdot Z + f(Y) \\ 0 \end{bmatrix} \quad (3.30)$$

with state vector

$$X = [G \quad X \quad S_1 \quad S_2 \quad Q_{sto} \quad Q_{gut} \quad Z \quad I_{add}] \quad (3.31)$$

and input vector

$$u = [u_{meal} \quad u_{ins} \quad Y] \quad (3.32)$$

and initial value conditions

$$\begin{bmatrix} G_0 \\ X_0 \\ S_{1,0} \\ S_{2,0} \\ Q_{sto,0} \\ Q_{gut,0} \\ Z_0 \\ I_{add,0} \end{bmatrix} = \begin{bmatrix} G_b \\ 0 \\ nV_I I_b T_d \\ nV_I I_b T_d \\ 0 \\ 0 \\ 0 \\ 0 \end{bmatrix} \quad (3.33)$$

where u_{ins} only corresponds to the constant basal insulin level $u_{ins} = u_b$. The initial conditions for the states is shown in equation 3.33, and correspond to a healthy person in a fasting state. The initial conditions for S_1 and S_2 is given in order to keep the basal insulin level at $u_b = nV_I I_b$.

The predicted blood glucose value from the simulation was compared to real blood glucose measurements. These blood glucose measurements was taken when a healthy person did the following test; a meal of 39 100 [mg] carbohydrates at $t=25$ and $t=236$, and a meal of 63 100 [mg] carbohydrates at $t=565$. At $t=570$, the person started an exercise session driving a spinning cycle machine for around 30 minutes. During exercise, there was no heart beat measurements. Therefore, the input Y was just set to a guessed value during the session. The parameter values were taken from the literature, and can be found in appendix.

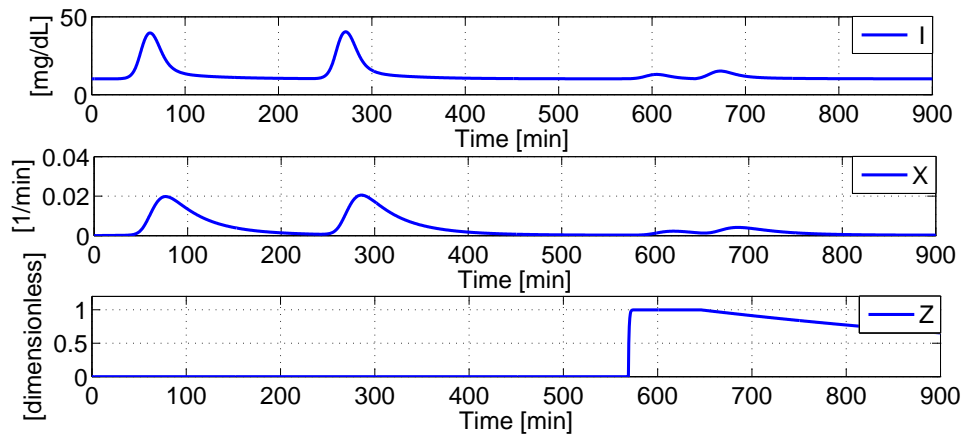


Figure 3.1: Insulin level

In figure 3.1 we can see how remote insulin X changes regarding to the insulin level I . As expected, the insulin level rises almost immediately after the meals, and there is some delay before the insulin appears in the intracellular space. After the third meal, which was followed by a exercise session, the insulin level doesn't rise that much. Exercise is suppose to increase insulin sensitivity, which means that not as much insulin is needed to decrease the plasma glucose level. In addition, the insulin independent glucose utilization increases, which result in a natural decrease in plasma glucose. The increased insulin sensitivity can be seen as the rise in Z during, and after exercise.

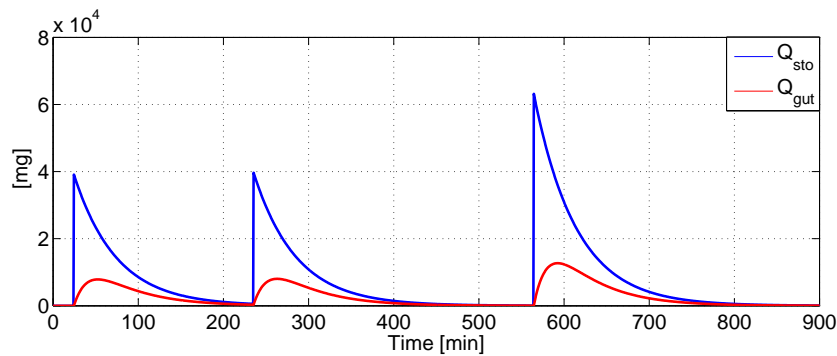


Figure 3.2: Level of glucose through the digestive system

The amount of glucose through the digestive system can be seen in figure 3.2. We can see that the amount of glucose in the gut is decreased and delayed compared to the amount of glucose in the stomach.

In figure 3.3, we can compare the predicted and real plasma glucose value. As we can see, the predicted output roughly follows the real data.

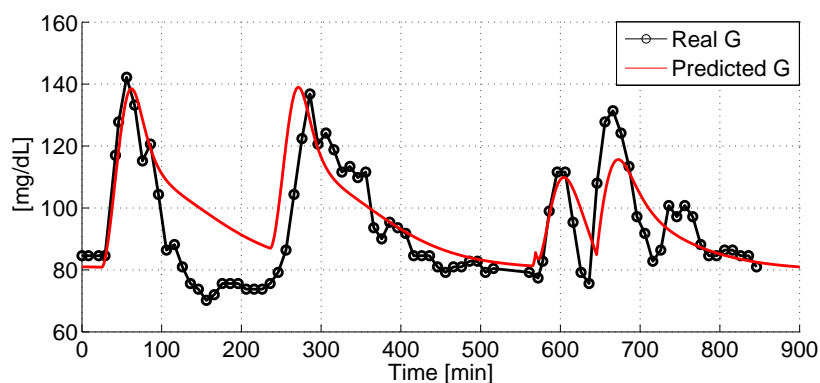


Figure 3.3: Real and estimated blood glucose

3.2.2 Simulation for a healthy person with Kalman filter

In order to improve the blood glucose prediction, a Kalman filter is used. The Kalman filter is an optimal state estimator, and is often used to estimate states from noisy data, or to estimate a state from different uncertain measurements, in order to estimate a state value that is closer to the real value. In our case, we want to improve the prediction by NIR and dielectric spectroscopy measurements.

The Kalman filter need a mathematical model of the system, which in the time discrete case can be described as [3]

$$x_{k+1} = f(x_k, u_k) + w_k \quad (3.34)$$

$$z_{k+1} = Hx_k + v_k \quad (3.35)$$

where H is a vector or matrix which gives the ideal connection between the measurement and the state vector. w_k is a vector with process noise and v_k is a vector of measurement error. Both w_k and v_k are assumed to be white noise processes with a known covariance structure

$$E[w_k w_i^T] = \begin{cases} Q_k, & i = k \\ 0, & i \neq k \end{cases} \quad (3.36)$$

$$E[v_k v_i^T] = \begin{cases} R_k, & i = k \\ 0, & i \neq k \end{cases} \quad (3.37)$$

$$E[w_k v_i^T] = 0, \text{ for all } k \text{ and } i \quad (3.38)$$

In order to relate an error to the estimated states \hat{x}_k^- , the estimation error is given in equation 3.39, with its corresponding error covariance matrix \bar{P}_k .

$$e_k^- = x_k - \hat{x}_k \quad (3.39)$$

$$\bar{P}_k = E[e_k^- e_k^{-T}] \quad (3.40)$$

Different types of Kalman filter exists to fit different kinds of models and applications. Due to the nonlinearity of the glucose model we need to use a linearized version of the Kalman filter, also known as the extended Kalman filter.

The Kalman Filter is actually a loop and is shown in figure 3.4, where a mathematical model of the system - together with measurements and covariance matrices, are used to calculate the Kalman gain. The Kalman gain is essential in calculating a predicted state, which is closer to the real state value. The loop starts with a prediction of the state \bar{x}_k and error covariance matrix \bar{P}_k , which is known as the a priori estimate. Then, the Kalman gain K , and the a posteriori state and error covariance matrix is calculated

$$K = \bar{P}_k H^T (H \bar{P}_k H^T + R)^{-1} \quad (3.41)$$

$$\hat{x}_k = \bar{x}_k + K(z_k - H\bar{x}_k) \quad (3.42)$$

$$P_k = (I - KH)\bar{P}_k(I - KH)^T \quad (3.43)$$

Then, the prediction of the a priori state and covariance matrix is updated

$$\bar{x}_{k+1} = f(\hat{x}_k, u_k) \quad (3.44)$$

$$\bar{P}_{k+1} = FP_kF^T + Q \quad (3.45)$$

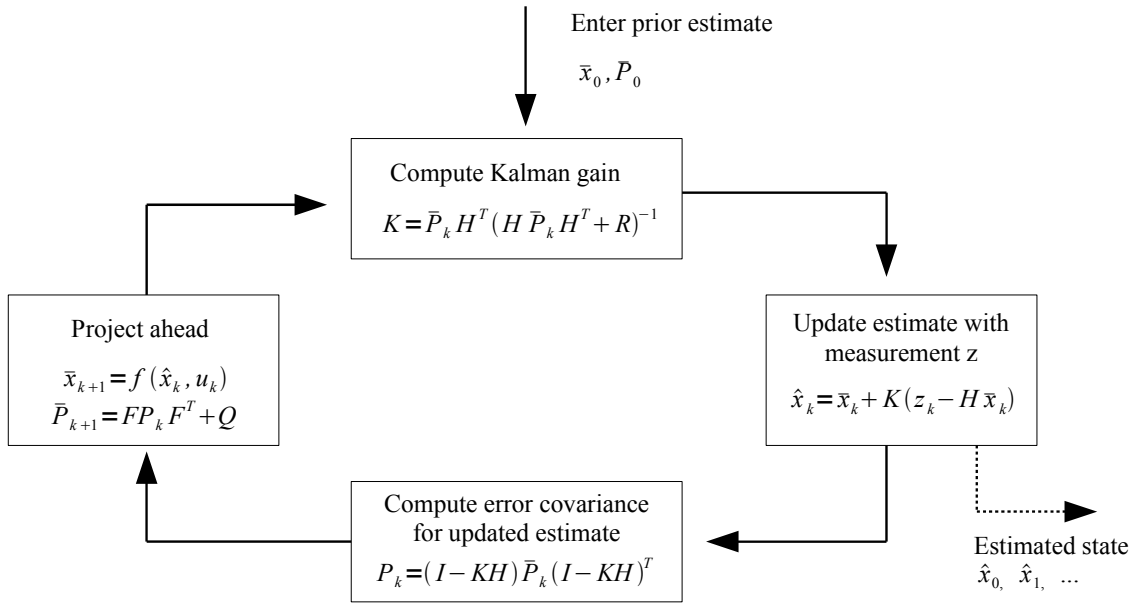


Figure 3.4: Extended Kalman filter loop

The matrix $F = \partial f / \partial x$ is the jacobian matrix, which is computed at each time step to linearize the non-linear function around the current estimate. The predicted, improved state which is the output of the system is \hat{x}_k . In most practical applications, the exact information of the covariance matrices Q and R are not known, and is often referred to as filter tuning parameters [23]. These matrices are found in the appendix together with the a priori estimate \bar{P}_0 . In our case, we only want the measure the blood glucose. Hence, H is a vector given as

$$H = [1 \ 0 \ 0 \ 0 \ 0 \ 0 \ 0 \ 0] \quad (3.46)$$

The Kalman filter was implemented for the same healthy person with the same model and input data as in section 3.1. The result can be shown in figure 3.5. Except from some deviations from the true value, especially at $t=490$, the predicted value of the blood glucose is highly improved. The result might be even further improved by tuning on the covariance of the process noise Q .

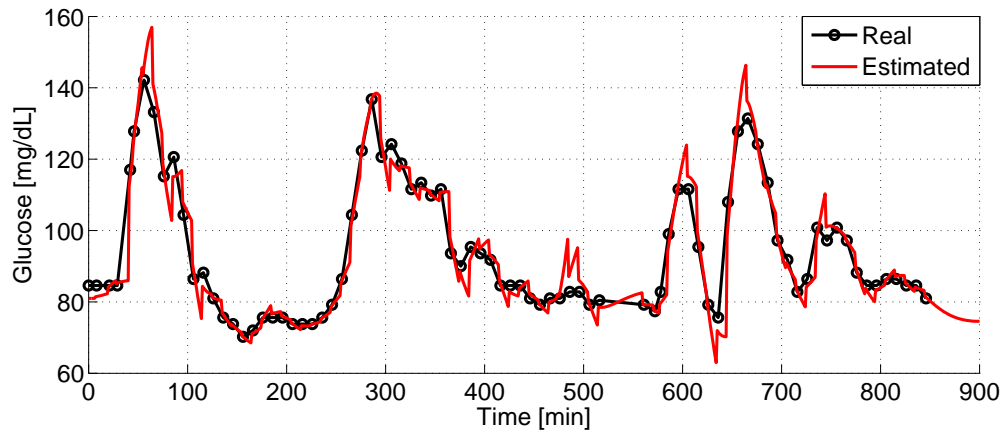


Figure 3.5: Real and simulated blood glucose with Kalman filter

Identifiability analysis

4

4.1 The system identification problem

In chapter 3, the model representing the glucose metabolism was introduced. Because it is desired to calibrate the model for each specific person to make the model as accurate as possible, there is a need for identifying the parameters in the model, which are stated in the parameter vector θ . To be able to estimate the parameter vector θ , we need to look at the theory of system identification. System identification have a wide application area, and are often needed in mathematical modeling. The overall goal of system identification is about estimating the parameters in order to minimize

$$\Phi = \sum_{i=1}^n [(\bar{y}_i - y_i)]^2 \quad (4.1)$$

where \bar{y} is the real signal, and y is the simulated system with estimated parameters. Hence, we want to find the parameter vector which makes the predicted value as close to the real value as possible. The parameters are estimated from known input and output data. When this data are known, the parameter vector θ can be estimated by various regression techniques, such as least square.

The parameter vector θ may represent the parameters of a black box model or parameters from another kind of structure. Therefore, the first step in system identification is actually to define a model which describes the system. Because the parameters are estimated from input and output data, we need to perform an experiment and measure certain outputs. When this is done, we are able to fit the model to the data by estimating the parameters. Afterwards, the model needs to be validated by comparing the real data and the model with the estimated parameter vector. If the validation fails, there is a need for designing another type of experiment or change the model, or both. This is shown in figure 5.4

The problem is that it may exist several parameter vectors θ which satisfy the relation between the given input and corresponding output for the model. In other cases, some of the parameters may be set to zero, even though this make no sense regarding the dynamics of the system. This can be explained by the identification properties of the model, which often explains why the validation fails or not. Following definitions to explain identifiability of a system is given in Ljung et al. (1994) [22]

Global identifiability: A system structure is said to be globally identifiable if for any admissible input $u(t)$ and any two parameter vectors θ_1 and θ_2 in the parameter space Θ , $y(u, \theta_1) = y(u, \theta_2)$ holds if and only if $\theta_1 = \theta_2$

Local identifiability: A system structure is said to be locally identifiable if for any θ within an open neighborhood of some point θ_* in the parameter space, $y(u, \theta_1) = y(u, \theta_2)$ holds if and only if $\theta_1 = \theta_2$

As indicated, we often distinguish between local and global identifiability. If the model is only local identifiable, there may exist several local solutions for the parameter vector θ , while global identifiability indicates the existence of only one unique θ . It is of course desired to find a unique parameter vector, but most often we are only able to find a local solution.

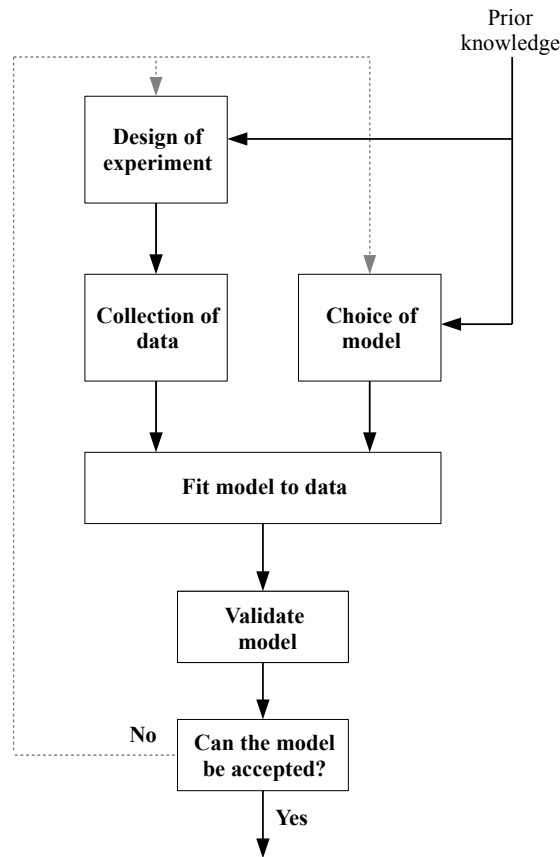


Figure 4.1: The parameter identification process

Because the parameter vector θ is estimated from the known input $u(t)$ and corresponding output $y(t)$, the identifiability properties will highly depend on the input vector. If $u(t)$ is constant during the whole experiment which corresponds to small changes in the output vector, it will most likely exist several parameter vector θ that satisfy the system. On the other hand, if $u(t)$ is varying which results in a varying output $y(t)$, it may only exist one unique parameter vector. Therefore, in order for a model to be identifiable, the input needs to be *persistent exciting*. This means that the input signal $u(t)$ need to change sufficiently in order to excite the system so that the experimental data contains enough information. When the system is sufficiently excited, the data contains enough information to estimate model parameters that con-

verge to their true values in a finite time. Hence, the performed experiment is crucial for the identification properties.

4.2 Identifiability analysis theory

Before the parameters in the glucose model can be estimated, there is a need to find a suitable parameter vector and check for the identifiability. Different methods for investigating the identifiability properties for a model are available in order to solve the system identification problem. These methods can also help us choosing an identifiable parameter vector θ for the system. The most common methods are structural identifiability analysis, practical identifiability analysis and sensitivity-based identifiability analysis.

4.2.1 Sensitivity-based analysis

With sensitivity analysis we can see how a model's output depends on variations in the parameter values. The model parameters have different impact on the output, where a small change in one parameter causes a huge change in the output, a change in other parameters might not affect the output at all. Hence, we can state the sensitivity of the output to each parameter in the model. Therefore, the analysis can be used to find which parameters are critical, and which parameters that have little effect on the output. If some parameters have little effect on the output, these parameters might be hard to identify and one may consider to do some changes in the given model. The sensitivity is quantified by calculating the variation in the output, with respect to changes in the q th component θ_q of the parameter vector θ . This can be defined in terms of partial derivatives and is often called the local sensitivity function. This is given by

$$s_{i,j}(t_k) = \frac{\partial y_i(t_k, \theta^*)}{\partial \theta_j} \quad (4.2)$$

where $s_{i,j}$ is known as the sensitivity coefficient and is calculated on each time step t_k for $k = 1, 2, \dots, N$. The system contains the state vector $X = [x_1 \ x_2 \ \dots \ x_d]$, and $y_i(t_k, \theta^*)$ is the measured output i for the system driven by the nominal parameter vector $\theta^* = [\theta_1^* \ \theta_2^* \ \dots \ \theta_q]$, and θ_j is a parameter component $\theta \in R^q$. The sensitivity matrix S for all time points consists of all the sensitivity coefficients, and is given as

$$S_{dN \times q} = \begin{bmatrix} s_{11}(t_1) & \dots & s_{1q}(t_1) \\ \vdots & \vdots & \vdots \\ s_{d1}(t_1) & \dots & s_{dq}(t_1) \\ \vdots & \vdots & \vdots \\ \vdots & \vdots & \vdots \\ s_{11}(t_N) & \dots & s_{1q}(t_N) \\ \vdots & \vdots & \vdots \\ s_{d1}(t_N) & \dots & s_{dq}(t_N) \end{bmatrix} \quad (4.3)$$

In practical applications, the sensitivity matrix can be calculated using the direct differential method, where the column sensitivity vector $S_j = \partial X / \partial \theta_j$ and the system

states are obtained simultaneously by solving the joint state and sensitivity profiles in equation 4.4, where $J = \partial f / \partial X$ is the Jacobian matrix, and $F_j = \partial f / \partial \theta_j$.

$$\begin{cases} \dot{X} = f(X, \theta, t), & X(t_0) = X_0 \\ \dot{S}_j = J \cdot S_j + F_j, & S_j(t_0) = 0 \end{cases} \quad (4.4)$$

How sensitive the output is with respect to different parameters, is described by the sensitivity coefficients. The larger the sensitivity coefficient are, the more notable the system response are with respect do the changes in parameters. If the system output is highly sensitive to a small perturbation of the parameter, the parameter is likely to be identifiable, otherwise, the parameter is likely to be unidentifiable. Since the local sensitivity function depends on both t and θ , the sensitivity is not constant. If the sensitivity s_q is close to zero on the time interval $[t - \delta, t + \delta]$ for θ in a neighborhood of the true value θ_0 , the model output is insensitive to the parameter θ_q at that particular time interval. However, same function s_q might take large values on a different time interval. Therefore, sensitivity analysis can also tell when each parameter has the greatest effect on the output.

The sensitivity analysis do not require actual experimental data to be performed, but enough information need to be given such that the model can be simulated. That requires a pre-specified parameter values θ^* , and a given input vector. In addition, the number and locations of measurements time points need to be defined. Then, equation 4.4 can be solved. Since the nominal parameter vector for the glucose model can take values from the literature, it is possible to perform sensitivity analysis for the glucose metabolism model to study the identification properties.

Sensitivity analysis is a rich topic, and different techniques based on the sensitivity matrix in 4.3, can be applied to investigate the identification properties of the system. It can be used to rank which parameters that affect the output the most, check for dependencies among parameters and used to state whether a model is identifiable or not. There is also a link between sensitivity analysis and practical identification methods, which make sensitivity analysis a key element in order to design an optimal experiment.

Local identifiability

In 4.2.1, parameter identifiability was studied according to the respective sensitivities for each parameter. Another way to check for identifiability is to consider the first order Taylor expansion of the system output near the pre-specified nominal parameter vector θ^* [19]:

$$y_k(\theta) = y(x(t_k), u(t_k), \theta) \quad (4.5)$$

$$y_k(\theta) \approx y(x(t_k), u(t_k), \theta^*) + \left. \frac{\partial y(x(t_k), u(t_k), \theta)}{\partial \theta} \right|_{\theta=\theta^*} \cdot \Delta(\theta - \theta^*) \quad (4.6)$$

where $k = (1, 2, \dots, N)$ denotes the index of the measurement time points. Let r_k

denote the error-free measurement $\Delta(\theta - \theta^*) = 0$ on each time step k . Then the residual sum of squares between the exact measurement and the linear approximation is

$$RSS(\Delta\theta) = \sum_{k=1}^N \left[r_k - y_k(\theta^*) + \left. \frac{\partial y(x(t_k), u(t_k), \theta)}{\partial \theta} \right|_{\theta=\theta^*} \cdot \Delta\theta \right]^2 \quad (4.7)$$

we assume that the parameters is estimated with a certian accuracy such that $r_k - y_k(\theta^*) = 0$, then

$$RSS(\Delta\theta) = \sum_{k=1}^N \left[\left. \frac{\partial y(x(t_k), u(t_k), \theta)}{\partial \theta} \right|_{\theta=\theta^*} \cdot \Delta\theta \right]^2 \quad (4.8)$$

which corresponds to

$$RSS(\Delta\theta) = (S\Delta\theta)^T \cdot (S\Delta\theta) \quad (4.9)$$

$RSS(\Delta\theta)$ represents the sum of squares that we of course want to equal zero. This can only be true if $S^T S \cdot \Delta\theta = 0$, which implies that $\Delta\theta = \theta - \theta^* = 0$, and that the estimated parameter vector $\hat{\theta}$ equals θ^* . This requires $S^T S$ to have full rank. Hence, the parameters are identifiable if S has full rank. Thus, it only states local identifiability, and is only valid near the pre-specified parameter vector θ^* . If $S^T S$ does not have full rank, there exists at least one non-trivial solution $\hat{\theta} \neq \theta^*$ such that the model parameters are not identifiable at θ^* .

Ranking of parameters

The sensitivity analysis enables us to plot how much different parameters affect the output. However, it can still be difficult to get an overview of which parameters that affect the output the most. Therefore, it is common to rank the parameters according to how much a given parameter influences the output.

Ranking the parameters can be done in different ways. In Miao et. al. (2011)[19], ranking of parameters is done by taking into consideration the *overall sensitivity*. It starts by normalizing the sensitivity matrix. Because the sensitivity function in 4.19 is simply output over input, it is sometimes difficult to attach meaning to the values. The absolute sensitivity can be useful for assessing the times at which parameter has its greatest or least effect, but is not ideal for comparing parameters. The normalized sensitivity function is dimensionless, and show which parameters that have the greatest effect on the output for a certain percent change in the parameters [14]. The normalized sensitivity coefficient are calculated as

$$s_{i,j}^i(t_k) = \frac{\theta_j}{y_i} \cdot \frac{\partial y_i(t_k, \theta^*)}{\partial \theta_j} \quad (4.10)$$

which forms the normalized sensitivity matrix

$$S_{dN \times q}^i = \begin{bmatrix} s_{11}^i(t_1) & \dots & s_{1q}^i(t_1) \\ \vdots & \vdots & \vdots \\ s_{d1}^i(t_1) & \dots & s_{dq}^i(t_1) \\ \vdots & \vdots & \vdots \\ s_{11}^i(t_N) & \dots & s_{1q}^i(t_N) \\ \vdots & \vdots & \vdots \\ s_{d1}^i(t_N) & \dots & s_{dq}^i(t_N) \end{bmatrix} \quad (4.11)$$

Then, the overall sensitivity can be obtained and expressed in terms of the dimensionless sensitivities coefficient [19]

$$os(\theta_j) = \sum_{k=1}^N \sum_{i=1}^d (s_{k,j}^i)^2 \quad (4.12)$$

where k is the time steps, and i represent each output $y = y_1, y_2, \dots, y_d$.

The larger the overall sensitivity parameter $os(\theta)$ for each parameter, the more sensitive the system response is with respect to small perturbations of this parameter.

4.2.2 Practical identifiability analysis

Identifiability analysis is often divided in structural identification analysis and practical identification analysis. For the structural identifiability analysis, also known as theoretical identifiability analysis, the analysis only depends on the model structure itself, and can be performed without the need of input and measured data. If the parameters in the model shows not be identifiable, the model structure itself needs to be changed to achieve identifiability. The analysis assumes that the model structure is absolutely accurate with exact measurements with no error. For nonlinear ODE, such as the glucose metabolism model, there exists different methods to state a structural identifiability. However, structural identifiability analysis is not usually performed [19], mostly due to computational complexity, and will not be performed here.

In the real world, the mathematical model is not exact and measurement errors will always be present. Therefore, all models need further practical identifiability analysis even though a theoretical analysis has been performed. Different methods can be used to state practical identifiability, where the most commonly used methods are Monte Carlo Simulation and to study Fischer Information Matrix (FIM).

The Monte Carlo simulation is used to evaluate whether the theoretically identifiable parameters can be reliably estimated with acceptable accuracy from noisy data [19]. This is done by determine the nominal parameter values, and solve the ODE model to get the output measurement. Afterwards, N sets of these measurements is generated, where measurement noise is added to each set. Then, the parameters is estimated for each set, and the relative estimation error is calculated for each parameter. If the relative estimation error for a given parameter is unacceptably high,

it is claimed that this parameter is not practically identifiable. Because this method required to estimate the parameters values, and the relative estimation error for each parameter, in each set N , this method is very computational demanding.

Fisher Information Matrix

The other approach is to calculate FIM, which is linked to the sensitivity analysis in chapter 4.2.1, where the FIM is calculated as follows

$$FIM = \sum_{k=1}^N (DS(t_k))^T Q^{-1} (DS(t_k)) \quad (4.13)$$

where matrix Q is a measurement-noise covariance matrix. The matrix $S(t_k)$ is the sensitivity matrix calculated for each time step k , and the matrix D is the measurement matrix. This result in a $q \times q$ matrix.

FIM is a measure of the information content of the measured signal relative to a particular parameter, and can therefore be used to quantify the richness of the experimental data. Hence, the FIM states the ability to estimate a specific set of parameters. The inverse of the FIM can also tell something about the identification properties, and is known as the Cramer-Rao bound . The Cramer-Rao bound is a lower bound on the error variance of the best estimator[12]. A solution with low bounds, results in a possible low mean squared error between the real and estimated data. Hence, a small Cramer-Rao bound corresponds to a more accurate result for the estimated parameters

The inverse of the FIM is also known as the covariance matrix C . With the covariance matrix make it possible to calculate the covariance between parameters in the parameter vector θ .

$$C = FIM^{-1} \quad (4.14)$$

Since the covariance is a measure on how much two variables change together, the covariance matrix can be used to state whether a parameter is identifiable or not. If there is a large covariance between two parameters, this indicates that the parameters will be hard to identify. This is because the parameter show the same behavior, and is therefore hard to distinguish. Because the covariance is calculated in different scales, the covariance are often hard to compare. Therefore, the correlation matrix is often used instead, which is the normalized covariance matrix. The correlation shows the dependency among the parameters, which is quantified between -1 and 1. A correlation of 1 means that the two variable are equal, and a correlation near 1 indicates that the two parameters is strongly dependent. Hence, if the correlation between two parameters is near 1, this may indicate non-identifiability. The correlation matrix R is

calculated in the following way

$$R = \begin{bmatrix} r_{11}(\theta_1, \theta_1) & r_{12}(\theta_1, \theta_2) & \dots & r_{1q}(\theta_1, \theta_q) \\ r_{21}(\theta_2, \theta_1) & r_{22}(\theta_2, \theta_2) & \dots & r_{2q}(\theta_2, \theta_q) \\ \vdots & \vdots & \ddots & \vdots \\ r_{q1}(\theta_q, \theta_1) & r_{q2}(\theta_q, \theta_2) & \dots & r_{qq}(\theta_q, \theta_q) \end{bmatrix} \quad (4.15)$$

where

$$r_{ij} = 1, \quad i = j \quad (4.16)$$

$$r_{ij} = \frac{C_{ij}}{\sqrt{C_{ii}C_{jj}}}, \quad i \neq j \quad (4.17)$$

As can be seen, the FIM is most important in its inverse form, where it reveals dependencies among parameters. Since the inverse is a measure in the lower bound of the error variance of the parameter estimates, this can be used directly in the design of an optimal experiment. In that case, a scalar measure of the covariance matrix is used by one of the following forms:

- A-optimal design: $\min(\text{Trace}(C))$
- D-optimal design: $\min(\det(C))$
- E-optimal design: $\min(\lambda_{\max}(C))$
- Modified E-optimal design: $\min((\lambda_{\max}(C)/\lambda_{\min}(C)))$

where $C = FIM^{-1}$. The A-optimal design tries to minimize the trace of C . However, this criterion is rarely used [9]. The D-optimal design tries to minimize the determinant of C , and results in the smallest volume of the confidence region in the parameter space. While E-optimal design corresponds to a minimization of the largest eigenvalue of the covariance matrix, and intends to minimize the maximum error. The modified E-optimal design minimizes the ratio of the largest to the smallest eigenvector. D-optimality and E-optimality is the most common methods [15].

To be invertible, the FIM should have a determinant different from zero and should not be ill-conditioned. To match these requirements, any pair of matrix columns should not be very similar. As each column of the matrix represents a parameter, the determinant of the FIM provides a reasonable measurement of the correlation of a set of parameters [31]. A large determinant value means lower values of the diagonal elements of the covariance matrix, which means a lower bound of the error variance. Hence, the Fisher Information Matrix is important regarding the identifiability of a model.

4.3 Identifiability analysis of the glucose model

In order to calibrate the glucose model, there is a need for identifying parameters by performing an experiment on each individual. In our case, all the parameters are known in advance, which means that not all parameters need to be estimated. Because the glucose model consist of 16 parameters, this would not have been possible with blood glucose as the only output. Therefore, we need to choose which parameters that seem reasonable to identify in order to make the model as accurate as possible.

In chapter 4.2.1, it was stated that sensitivity analysis plays an important role in finding a suitable parameter vector. This is also true in our case, but we also have to take the glucose-insulin interaction theory from chapter 2.2.1 into consideration. If we put all the parameters in the parameter vector we get the following

$$\theta = \left[G_b \quad I_b \quad p_1 \quad p_2 \quad p_3 \quad T_i \quad V_p \quad V_I \quad \frac{1}{T_d} \right. \\ \left. C_1 \quad a_1 \quad k_{emp} \quad k_{abs} \quad f \quad HR_b \quad \alpha \quad \beta \quad a \quad T_{ex} \right]$$

Because certain body fluids have known volumes, the parameters V_p and V_I which represents the plasma and insulin distribution space, can be assumed known. The basal glucose G_b and basal insulin I_b for a healthy person, can be found by blood measurements after a fasting state. These basal values can also be found for a diabetic by skipping activities that would alter their blood glucose such as eating, exercise and bolus insulin. Then, use a blood glucose monitor to check the amount of insulin needed to keep the blood glucose in a specific range [10]. For the basal heart rate HR_b , this can be found by simple measuring the resting heart rate. Hence, there is no need to use parameter estimation techniques to estimate these parameters. Because the pancreatic insulin secretion function is only valid for a healthy person, the parameters C_1 and a_1 may be disregarded from the parameter vector.

Intuitive, it may seem reasonable to identify those parameters that varies the most among individuals. However, the rate of biochemical processes in our bodies depends on age, gender, external temperature, genetics, body fat percentage and weight. Hence, most likely all parameters in the glucose model is individual. Therefore, the model and its parameters need further study. We are left with the following vector of parameters which we want to take closer look upon:

$$\theta = \left[p_1 \quad p_2 \quad p_3 \quad \frac{1}{T_d} \quad \alpha \quad \beta \quad a \quad k_{abs} \quad k_{emp} \quad T_i \quad f \quad T_{ex} \right] \quad (4.18)$$

4.3.1 Ranking of parameters with different experiments

Sensitivity analysis might give us a clue for which parameters that should be included in the parameter model, where the parameters that have little influence on blood glucose perhaps should be removed. The sensitivity of the glucose output to the different parameters, depends on the experimental data. For example, if there is no carbohydrate intake during an experiment, the glucose concentration will be insensitive to the parameters k_{emp} and k_{abs} .

A sensitivity analysis for the glucose model could give us an indication in which parameters that affect the glucose output, and when. Therefore, two different experiments representing a healthy person were simulated, and the sensitivity was calculated for the parameter vector 4.18. The model was simulated in Matlab, where the jacobian matrix $\partial f/\partial x$ was calculated numerically, while $\partial f/\partial \theta$ was found as

$$\frac{\partial f}{\partial \theta} = \begin{bmatrix} \frac{\partial f_1}{\partial \theta_1} & \dots & \frac{\partial f_1}{\partial \theta_q} \\ \vdots & \ddots & \vdots \\ \frac{\partial f_d}{\partial \theta_1} & \dots & \frac{\partial f_d}{\partial \theta_q} \end{bmatrix}$$

$$\frac{\partial f}{\partial \theta} = \begin{bmatrix} G_b - G & 0 & 0 & 0 & -XZG & -YG \\ 0 & -X & I - I_b & p_3 T_i S_2 / V_I & 0 & 0 \\ 0 & 0 & 0 & -S_1 & 0 & 0 \\ 0 & 0 & 0 & S_1 - S_2 & 0 & 0 \\ 0 & 0 & 0 & 0 & 0 & 0 \\ 0 & 0 & 0 & 0 & 0 & 0 \end{bmatrix}$$

$$\left[\begin{array}{cccccc} 0 & f Q_{gut} / V_p & 0 & 0 & k_{abs} Q_{gut} / V_p & 0 \\ 0 & 0 & 0 & (p_3 / V_I)(S_2 / T_d + I_{own}) & 0 & 0 \\ 0 & 0 & 0 & 0 & 0 & 0 \\ 0 & 0 & 0 & 0 & 0 & 0 \\ 0 & 0 & -Q_{sto} & 0 & 0 & 0 \\ 0 & -Q_{gut} & Q_{sto} & 0 & 0 & 0 \\ dZda & 0 & 0 & 0 & 0 & Z / T_{ex}^2 \end{array} \right]$$

where

$$dZda = \frac{(1 - Z)f(Y)(1 - f(Y))}{a} \quad (4.19)$$

and

$$I_{own} = \frac{Rm}{1 + \exp((C_1 - G)/a_1)} \quad (4.20)$$

where 4.20 is zero for a diabetic type 1 person.

Healthy person

In experiment one, a meal of 50 000[mg] carbohydrates were taken at t=50, with a following 30 minutes exercise session at t=150. In the second simulation, a meal of 40 000 [mg] carbohydrates were taken at t=30 and a meal of 50 000[mg] of carbohydrate was taken at t=150. At t=60, a 30 minutes exercise session started. The duration of all simulations were 500 minutes, and with a constant heart rate $HR = 120$ during exercise.

The sensitivities was plotted for the first experiment and can be seen in figure 4.2, 4.3 and 4.4. For parameter p_1 , the glucose level is most affected during the meal and

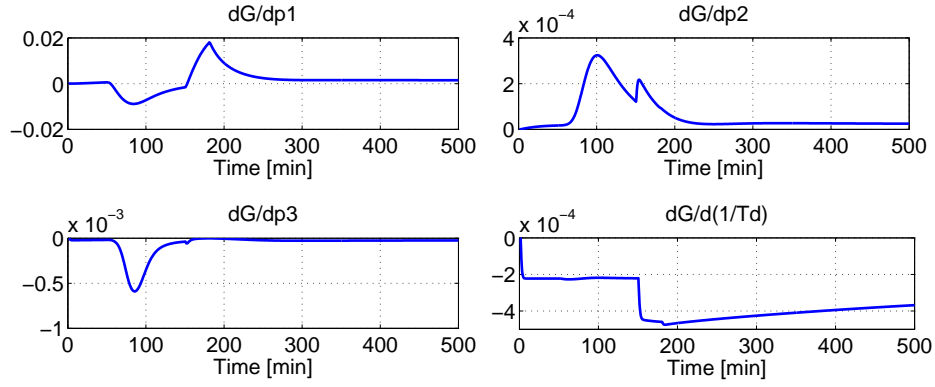


Figure 4.2: Sensitivity for parameters 1 to 4

exercise. The same is also true for parameter p_2 . Parameter p_3 is only influencing the glucose level during the meal. As can be seen, time constants T_d and T_i are the only parameters which affect the glucose level in the fasting state.

As expected, plasma glucose is only influenced by parameters k_{abs} , k_{emp} and f after the meal. After about 250 minutes, glucose is not affected by these parameters at all, which indicates that all the glucose has passed through the digestive system.

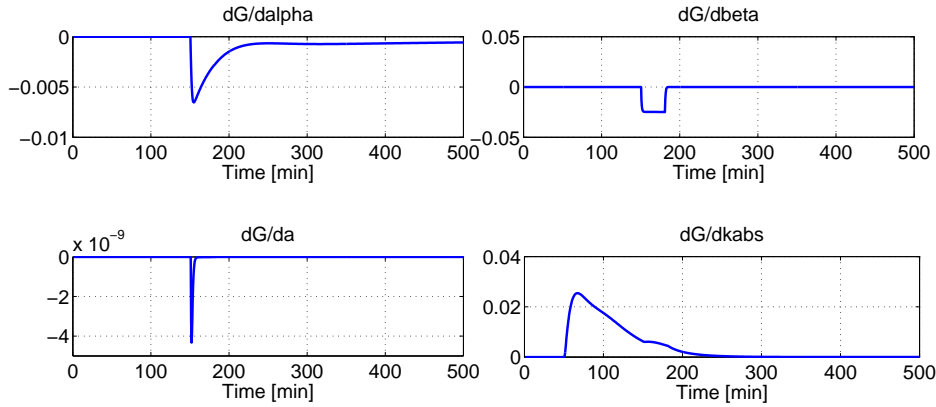


Figure 4.3: Sensitivity for parameters 5 to 8

We can see that the glucose level is not influenced by the exercise parameters α , β , a and T_{ex} until the start of the exercise session at $t=180$, which is true because $Z = 0$ when $HR = HR_b$. The parameter β which describes the insulin independent glucose utilization during exercise, is only influencing the glucose level during the exercise. The parameter α which describes the increased insulin sensitivity, affect the blood glucose level both during and after exercise. As can be seen, the time constant T_{ex} seems to have a small influence the glucose level.

From the plots, it can be seen that the glucose output is affected by the different parameters at different time slots depending on input u_{meal} and the exercise describing input Y . To see which parameters that totally have most effect on the glucose level, the parameters were ranked according to equation 4.12. The rankings are shown in table 4.1 for both experiment one and two. The parameters are ranked based on sensitivity calculations every 30 seconds to give an overall view.

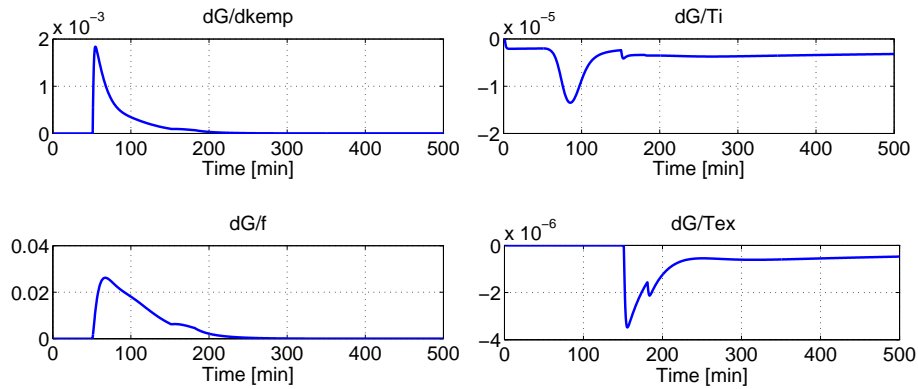


Figure 4.4: Sensitivity for parameters 9 to 12

Diabetic type 1 person

Two simulations were also done in the case of a diabetic type 1 person. In the first simulation an insulin injection of 3U was taken at $t=50$, followed by meal of 50 000 [mg] of carbohydrates at $t=60$. At $t=150$ a 30 minutes exercise session started. In the second simulation started with an exercise session of 30 minutes at $t=30$. A meal of 65 000 [mg/min] of carbohydrates was taken at $t=100$, followed by an insulin injection at $t=110$ of 3U.

How much fast-acting insulin that is needed for a diabetic person after eating meal of carbohydrates, is highly individual. A rule of thumb is that 1U of insulin for every 10-18 grams of carbohydrate. However, for a very young child, as little as 0.1U of fast-acting insulin might cover 15 grams of carbohydrate. Therefore, the size of the insulin injection inputs are varying, but are chosen in such a way that 1U is supposed to cover 10-18 grams of carbohydrates.

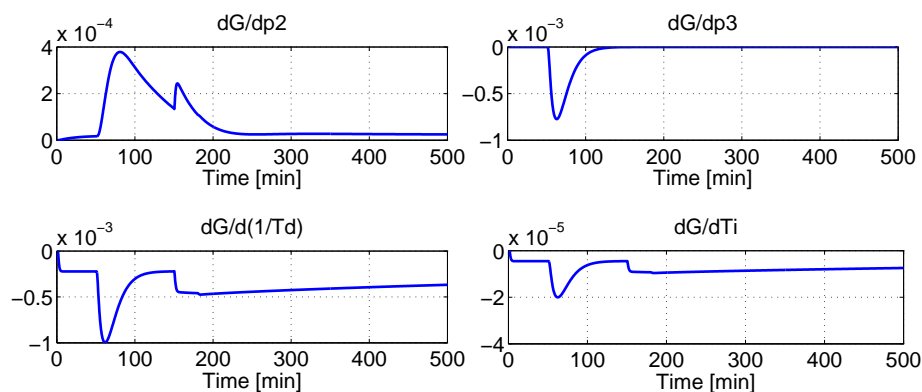


Figure 4.5: Sensitivity for a diabetic type 1 person

Because the first simulation was quite similar to the first simulation for the healthy person, not all sensitivities were plotted. The most interesting with this simulation was the time constant T_d which is the delay for the subcutaneous insulin injection. This parameters is plotted in figure 4.5 together with the sensitivities regarding p_2 , p_3 and T_i . In this simulation, the output glucose is affected more by T_d the moment

after the insulin injection. The same is true for parameter T_i , while both parameter p_2 and p_3 show the same behavior as for the healthy person.

The overall sensitivity ranking was computed for both simulations and is shown in table 4.1. The parameters show the same tendencies in all experiments, for both a healthy and a diabetic type 1 person. For all experiments, the glucose level is quite insensitive to the parameters a , T_i and T_{ex} . The glucose level seems to be most affected by parameters f and k_{abs} . The glucose level is also highly affected by parameter β , but also of parameter α . We can see that the glucose level was particular affected by parameter α in simulation 2 for both the case of a healthy and a diabetic type 1 person. In these simulations, a meal was taken after the exercise session, where the increased insulin sensitivity caused by parameter α results in an increase in overall sensitivity. The remaining parameters do not seem to have a huge impact on the glucose output.

Table 4.1: Overall sensitivity for healthy and diabetic type 1 person

Parameter	Simulation 1 (healthy)	Simulation 2 (healthy)	Simulation 1 (diabetic)	Simulation 2 (diabetic)
p_1	243.80	77.18	176.66	196.85
p_2	0.10	0.19	0.16	0.55
p_3	0.16	0.32	0.26	1.27
$\frac{1}{T_d}$	1.37	1.50	1.78	3.14
α	18.40	155.83	23.01	455.91
β	368.34	366.51	336.79	371.10
a	6.27E-13	8.67E-13	7.88E-13	9.96E-15
k_{abs}	603.28	1236.40	838.52	1493.10
k_{emp}	0.97	1.69	1.27	2.06
T_i	1.87E-4	3.17E-4	2.36E-4	7.49E-4
f	639.95	1311.60	889.51	1583.90
T_{ex}	7.14E-6	9.57E-5	8.76E-6	3.12E-4

4.3.2 Calculating the covariance matrix

In the previous section, a sensitivity analysis was performed and the parameters were ranked according to the parameter vector

$$\theta = \left[p_1 \quad p_2 \quad p_3 \quad \frac{1}{T_d} \quad \alpha \quad \beta \quad a \quad k_{abs} \quad k_{emp} \quad T_i \quad f \quad T_{ex} \right] \quad (4.21)$$

If we calculate the rank of the $S^T S$ matrix for the simulations of a healthy person described in section 4.3.1, where a simple meal was followed by an exercise session, we find that the rank equals 9 for all simulations when the glucose output is assumed measured every 15 minute. There may exist an input vector that increases the rank, but the results indicate that the parameter vector in 4.21 is not identifiable. Hence, it not possible to find a unique, local parameter vector.

As stated in section 4.2.2, the correlation matrix can tell something about the dependencies among parameters. If two parameters show the same behavior in a

model, these two parameters might be difficult to distinguish by parameter identification techniques. Therefore, the correlation matrix can show where identifiability might be a problem. The correlation was calculated by equations 4.15, 4.16 and 4.17 according to the first simulation described in section 4.3.1 for a healthy person. The result is shown in table 4.2. The FIM was found by assuming a glucose measurement every 15 minutes. Another experiment, or another glucose measurement time, would have given a different result.

Table 4.2: Correlation matrix for a healthy person

1.0000	-0.5575	0.6932	-0.1465	-0.5227	-0.4175	-0.4389	-0.6876	-0.5353	0.1797	-0.6878	-0.5041
-0.5575	1.0000	-0.7927	-0.4941	-0.1795	-0.1272	-0.0913	0.7878	0.4994	-0.7080	0.7883	-0.1590
0.6932	-0.7927	1.0000	0.3875	0.0779	0.0173	0.0039	-0.8584	-0.6251	0.7140	-0.8587	0.0811
-0.1465	-0.4941	0.3875	1.0000	0.8178	0.2669	0.2207	-0.3867	-0.3113	0.9221	-0.3868	0.8545
-0.5227	-0.1795	0.0779	0.8178	1.0000	0.6141	0.5898	-0.0367	-0.0166	0.6538	-0.0367	0.9572
-0.4175	-0.1272	0.0173	0.2669	0.6141	1.0000	0.8533	-0.0524	-0.0238	0.2099	-0.0525	0.3860
-0.4389	-0.0913	0.0039	0.2207	0.5898	0.8533	1.0000	-0.0347	-0.0157	0.1692	-0.0347	0.4524
-0.6876	0.7878	-0.8584	-0.3867	-0.0367	-0.0524	-0.0347	1.0000	0.8988	-0.6540	1.0000	-0.0223
-0.5353	0.4994	-0.6251	-0.3113	-0.0166	-0.0238	-0.0157	0.8988	1.0000	-0.4988	0.8984	-0.0100
0.1797	-0.7080	0.7140	0.9221	0.6538	0.2099	0.1692	-0.6540	-0.4988	1.0000	-0.6542	0.6830
-0.6878	0.7883	-0.8587	-0.3868	-0.0367	-0.0525	-0.0347	1.0000	0.8984	-0.6542	1.0000	-0.0223
-0.5041	-0.1590	0.0811	0.8545	0.9572	0.3860	0.4524	-0.0223	-0.0100	0.6830	-0.0223	1.0000

It is also interesting to see if the correlation matrix will change when exogenous insulin is added. Therefore, the correlation matrix was also calculated for the first simulation described in section 4.3.1 for a diabetic type 1 person. The result is shown in table 4.3. The FIM was found by assuming a glucose measurement every 15 minutes.

Table 4.3: Correlation matrix for a diabetic person

1.0000	-0.2196	0.0138	-0.3428	-0.6647	-0.4414	-0.5419	-0.3149	-0.2430	-0.3411	-0.3150	-0.7586
-0.2196	1.0000	-0.5652	-0.6360	-0.3026	-0.2742	-0.1895	0.9633	0.8795	-0.6395	0.9633	-0.2397
0.0138	-0.5652	1.0000	0.5540	0.0009	0.0013	0.0005	-0.4676	-0.5574	0.5540	-0.4672	0.0003
-0.3428	-0.6360	0.5540	1.0000	0.5971	0.2371	0.1923	-0.4642	-0.4423	1.0000	-0.4641	0.6675
-0.6647	-0.3026	0.0009	0.5971	1.0000	0.8017	0.7622	-0.1531	-0.0825	0.5967	-0.1532	0.9285
-0.4414	-0.2742	0.0013	0.2371	0.8017	1.0000	0.8399	-0.1719	-0.0932	0.2369	-0.1720	0.5623
-0.5419	-0.1895	0.0005	0.1923	0.7622	0.8399	1.0000	-0.1133	-0.0607	0.1922	-0.1134	0.6694
-0.3149	0.9633	-0.4676	-0.4642	-0.1531	-0.1719	-0.1133	1.0000	0.9445	-0.4692	1.0000	-0.1022
-0.2430	0.8795	-0.5574	-0.4423	-0.0825	-0.0932	-0.0607	0.9445	1.0000	-0.4482	0.9443	-0.0544
-0.3411	-0.6395	0.5540	1.0000	0.5967	0.2369	0.1922	-0.4692	-0.4482	1.0000	-0.4690	0.6670
-0.3150	0.9633	-0.4672	-0.4641	-0.1532	-0.1720	-0.1134	1.0000	0.9443	-0.4690	1.0000	-0.1022
-0.7586	-0.2397	0.0003	0.6675	0.9285	0.5623	0.6694	-0.1022	-0.0544	0.6670	-0.1022	1.0000

Because of the size of the table, it might be a bit hard to compare the different parameters. However, a close look indicates that there is no big differences between the two correlations matrices. It can be seen in both tables that the correlation is strong between certain parameters. In our case, if the correlation between two parameters is strong, we can choose between changing the model to avoid the identifiability problem, or simply just add one of the two parameters to the parameter vector, and simply find the other parameter value from the literature. In the following we will look closer to the correlation among the different parameters.

The correlation among the parameters in the exercise model is strong. A correlation of 1 is found between parameters k_{abs} and f , and the correlation between k_{empt}

and f , and k_{abs} and k_{emp} , is both over 0.89. The only input affecting the gut submodel is the input u_{meal} . No other input will possibly have any influence on the dynamic of the gut submodel, which means that the identifiability of these parameters can not be improved by exciting the system by other inputs. Even though exciting the system with several meals, the parameters are still correlated. Hence, it most likely not possible to separate parameter k_{abs} and f . Therefore, one of these two parameters might need to be taken from the literature, or the model needs to be changed in order to avoid the identifiability problem.

Among the parameters in the exercise model, the strongest correlation is 0.9572 and is found between parameters α and T_{ex} . There is also a correlation of 0.8533 between β and a . As can be seen from the sensitivity plots, the glucose level to not show the same sensitivity behavior regarding parameters β and a .

In the case for the diabetic person, it seems to be strong correlations between k_{abs} and p_2 , and k_{empt} and p_2 . In addition, a strong correlation is also seen between $1/T_d$ and T_i .

4.3.3 Comparing different parameter vector by using the Fishers Information Matrix

In section 4.2.2, it was stated that an optimal experiment could be found by minimizing the determinant of the inverse of the FIM. Minimizing this criteria maximizes the expected accuracy of the parameter estimates. In order to find the parameter vector that maximized the accuracy of the parameter estimates, optimal experiments could be calculated for all combinations of parameter vectors. Then, the parameter vectors could be compared, and parameter combinations could be disregarded based on the results. However, all possible combinations for a parameter vector of size k are found by the binomial coefficient given as

$$C_k = \frac{n!}{(n-k)!k!} \quad (4.22)$$

where n is the number of parameters to choose from. Hence, if we want to find all combinations for a parameter vector of size 6 when there is a total of 12 parameters to choose from, this corresponds to a 924 different combinations. Hence, solving an optimal experiment for each parameter combination is too computational demanding.

In order to compare the identifiability properties of parameter vectors of different sizes, 14 different experiments was simulated. In each experiment, the D-optimality value $\det(C)$ was calculated for all possible combinations of parameter vectors of size six, seven and eight parameters. The value was calculated corresponding to blood glucose measurements every 10, 20, 30 and 40 minutes. In order to compare the different parameter vectors, the Fisher Information Matrix was calculated based on a normalized sensitivities.

In addition to the D optimal criteria, the rank of the $S^T S$ matrix was calculated to state identifiability or not. The experiments were designed to contain one or two meals, and a 20 minutes exercise session corresponding to a heart rate of 132[beat/s/min]. In the case of a diabetic person, insulin was injected before or after the meal, or a small dose was given both before and afterwards. Because it is limitations in the

duration and how the experiment possibly can be performed, 14 different simulations seemed like an adequate number to reveal the dynamic of the model.

From the ranking of parameters in section 4.3.1, both parameters parameter T_i and T_{ex} showed to have a very small impact on the glucose output. Therefore, to reduce the complexity of the calculations, these two parameters were disregarded. This means that the ten parameters $[p_1 p_2 p_3 1/T_d \alpha \beta a k_{abs} k_{emp} f]$ were used to combine different parameter vectors.

The calculation of the D-optimality value showed, in general, that the same parameter vector combinations minimized the D-optimality value for all 14 simulations. Therefore, the results in table 4.4 only shows the D-optimality value calculated for simulation 13, where a meal was taken in the early beginning of the experiment, followed by an exercise session after about 130 minutes.

Table 4.4: Parameter vector of size 3 for healthy person

Parameter vector θ	$T = 10$	$T = 20$	$T = 30$	$T = 40$
$[\alpha \beta f]$	1.0233e+16	6.1571e+16	2.3106e+17	6.2632e+17
$[p_1 \alpha f]$	1.0266e+16	5.2782e+16	1.0398e+17	3.8245e+17
$[p_2 p_3 a]$	1.0067e+37	5.5132e+37	2.4897e+38	2.0600e+38
$[p_2 p_3 k_{emp}]$	8.8228e+35	4.7378e+36	4.6051e+37	4.1652e+39

Table 4.5: Parameter vector of size 3 for diabetic person

Parameter vector θ	$T = 10$	$T = 20$	$T = 30$	$T = 40$
$[\alpha \beta f]$	3.2262e+16	6.7952e+17	6.9953e+17	2.1287e+18
$[p_1 \alpha f]$	2.8617e+16	1.3975e+17	2.8046e+17	9.4991e+17
$[p_2 p_3 a]$	4.0596e+36	3.7890e+37	2.5470e+37	1.2832e+38
$[p_2 p_3 k_{emp}]$	2.5495e+35	1.9030e+36	8.0547e+38	1.1086e+40

In table 4.4, we can see the lowest and highest value of the D-optimality value for a parameter vector of size 3. We can see the value increases with an increase in supposed glucose measurement times, which is true because fewer glucose measurements result in a FIM matrix which contain less information about the system. We can see that $[\alpha \beta f]$ produces the lowest values for all sampling times. This is also true in the case of a diabetic type 1 person, which is shown in table 4.5. The parameter vector combinations which corresponds to the one with the lowest and highest value of the D-optimality value, are equal for both a diabetic type 1 person and a healthy person. In addition, the calculated value of the D-optimality value is quite similar in both cases.

The results in the case of a parameter vector of size 6 is shown in table 4.6 in the case of a healthy person, and in 4.7 in the case of a diabetic type 1 person. Again, the parameter vector combinations for both a diabetic type 1 person and a healthy person seem to show the same results.

Therefore, only one parameter vector combination for a parameter vector of size 8, has proved full rank of the $S^T S$ matrix. In some experiments it did not prove full

Table 4.6: Parameter vector of size 6 for healthy person

Parameter vector θ	$T = 10$	$T = 20$	$T = 30$	$T = 40$
$[p_1, 1/T_d, \alpha, \beta, k_{emp}, f]$	1.1898e+42	3.7467e+43	4.1240e+46	5.0946e+48
$[p_1, 1/T_d, \alpha, \beta, k_{abs}, k_{emp}]$	2.8509e+44	8.9778e+45	9.8676e+48	1.2183e+51
$[p_1, p_2, p_3, 1/T_d, \beta, k_{emp}]$	5.3304e+58	2.3792e+60	9.7178e+61	1.0945e+66
$[p_1, p_2, p_3, 1/T_d, k_{abs}, k_{emp}]$	7.4035e+58	5.6762e+60	3.0532e+63	4.9064e+67

Table 4.7: Parameter vector of size 6 for diabetic person

Parameter vector θ	$T = 10$	$T = 20$	$T = 30$	$T = 40$
$[p_1, 1/T_d, \alpha, \beta, k_{emp}, f]$	1.7192e+42	4.5279e+43	4.4174e+48	7.8674e+50
$[p_2, 1/T_d, \alpha, \beta, k_{abs}, k_{emp}]$	5.6950e+48	7.8742e+50	8.2766e+52	6.7586e+58
$[p_1, p_2, p_3, 1/T_d, \beta, k_{emp}]$	1.0369e+58	6.0479e+59	8.4828e+62	1.0178e+69
$[p_1, p_2, p_3, 1/T_d, k_{abs}, k_{emp}]$	1.3548e+59	1.9299e+61	3.0595e+65	2.7894e+71

rank for a glucose measurement every 30 and 40 minutes. In the case of parameter vector of size 9, only one parameter vector proved to have full rank in the case of glucose measurement every 10 and 20 minutes.

It can be seen that the different parameter vector combinations for both a healthy and diabetic type 1 person, have the almost the same calculated D-optimality value. Hence, a chosen parameter vector of a certain size will show almost the same identifiability properties for both a healthy and a diabetic type 1 person. How the D-optimality criterion changes with different sizes of the parameter vector, is shown in table 4.8. The calculation is done in the case of a healthy person.

Table 4.8: Overview of parameter vector with lowest optimality criterion for healthy person

Size of parameter vector	Lowest $\det(C)$ for $T = 20$	Parameter vector
2	1.5769e+09	$[\alpha, f]$
3	5.2782e+16	$[p_1, \alpha, f]$
4	2.2218e+24	$[p_1, \alpha, \beta, f]$
5	4.4816e+33	$[p_1, \alpha, \beta, k_{emp}, f]$
6	4.5279e+43	$[p_1, 1/T_d, \alpha, \beta, k_{emp}, f]$
7	2.3929e+56	$[p_1, p_2, 1/T_d, \alpha, \beta, k_{emp}, f]$
8	1.0764e+72	$[p_1, p_2, p_3, 1/T_d, \alpha, \beta, k_{emp}, f]$
9	-	-

In order to get an overview of the column rank of the $S^T S$ matrix, the rank was calculated for all combinations of all sizes of the parameter vector. In the case of parameter vector of size 9, no vectors proved to have full column rank for all four glucose measurement times. It was also revealed that parameter vectors containing a were not identifiable when the size of the parameter vector was five or higher.

Table 4.9: Overview of rank for a healthy person

Size of parameter vector	Number of combinations with full coulum rank	Comments
2	38	
3	83	
4	108	
5	91	Parameter a no longer identifiable
6	49	
7	15	
8	2	
9	0	

The differences between the vector with the lowest and highest value of the D-optimality value, have shown that the choice of parameter vector is important for accuracy of the parameter estimates. It has also been shown that parameter a is only identifiable if the size of the parameter vector is four, or lower. In addition, parameter vectors containing a have shown poor values of the D-optimality criterion.

4.4 Summary

The sensitivity analysis shows that the parameters a , T_i and T_{ex} have a very small influence on the blood glucose output. Because of its small influence on the output, this parameters are hard to identify. In addition, one may question the reason for identifying a parameter which does not have any affect on the output. The practical analysis, shows strong correlations between a and α , and a and β . Parameter T_i shows s strong correlation to both T_d and p_2 , while T_{ex} is highly correlated with T_d and α . The rank of the $S^T S$ matrix, showed that no parameter vectors of size 5 or higher, containing parameter a , were identifiable. In addition, calculating the D-optimality criterion showed that parameter vector containing a , the D-optimality value was much higher. Hence, this parameter is not suited for parameter identification.

The sensitivity analysis also shows that parameters k_{abs} , f , α , β and p_1 have a huge influence on the glucose output. Identifying these parameter will be of great importance of the accuracy of the model. However, the practical analysis shows strong correlations among the parameters. The practical analysis shows a correlation of 1 between k_{abs} and f , which means that it will be practically impossible to separate these two parameters. In addition, they are both highly correlated to parameter k_{emp} . Hence, most likely only one of these parameters can be identified. Both k_{abs} and f also show strong correlations to parameters p_2 and p_3 . In the case of a healthy person, there is also a strong correlation between p_1 and p_3 , and p_2 and p_3 . This may suggest that p_3 should not be identified. In the case of a diabetic person, there is also s strong correlation between k_{emp} and p_2 . In the case of a healthy person, there seem to be some correlation between $1/T_d$ and α .

Calculation of the D-optimality value, shows that the accuracy of the estimated parameters highly depend on the choice of parameter vector. As expected, the value increases with an increase between each glucose measurement. How much this in-

crease means in practice, is a bit hard to say. However, the glucose measurement sampling time, should perhaps not be constant.

If k_{emp} is not calculated by a function, but need to be identified, k_{abs} and f can most likely not be a part of the parameter vector. Taken into consideration the correlation between α and $1/T_d$, this means that parameters p_1 , p_2 , $1/T_d$, β and k_{emp} is a vector set without strong correlations.

Calibration and choice of parameter vector based on real glucose data

5

5.1 RDE criterion

Until now we have analyzed the model regarding its identifiability properties. We have looked at the ranking of parameters to state which parameters affect the glucose output the most, and we have calculated the D-optimality criteria and compared different parameter vectors of different sizes. Even with all this information, we still don't know how many parameters that should be added to the parameter vector. Even though the theoretical analysis have showed which parameters that may be added - will the estimation of parameters work in practice? The glucose model is only an approximation of the process, and blood glucose measurement meters are known for occasionally incorrect readings. Therefore, the error between the glucose measurements and the estimated may become large. A natural step might be to look at real glucose data.

Inspired by a method given in Machada et. al. (2008)[31], we might be able to get a better overview of the identifiability regarding the number of possible parameter vector combinations. The method is based on what is called the RDE-criterion, which is given as [31]:

$$RDE = \frac{normD}{modE} \quad (5.1)$$

It was stated that the covariance matrix $C = FIM^{-1}$ represented the lower bound on the error variance of the best estimator. Therefore, we wanted $det(C)$ to be as low as possible. In this case, normD is given as the normalized determinant of the FIM

$$normD = D \|\theta\|^2 \quad (5.2)$$

where

$$D = det(FIM) \quad (5.3)$$

and $\|\theta\|$ is the Euclidean norm. Since we want the lower bound of the error variance of the estimator to be as low as possible, we want normD as big as possible. The normalization able us to compare normD for different subsets. For modE, this is defined as the ratio between the highest and the lowest FIM eigenvalue

$$modE = \frac{\max(\lambda_{FIM})}{\min(\lambda_{FIM})} \quad (5.4)$$

A modE criterion close to unity indicates that all the involved parameters independently affects the outputs. Because normD gives an indication of how good the estimator may perform, and modE represents the dependencies among parameters, both normD and modE are interesting parameters. Calculating the ratio of normD and modE gives us the RDE, which we want to be as large as possible and work as an index to compare the different combinations of parameter vectors.

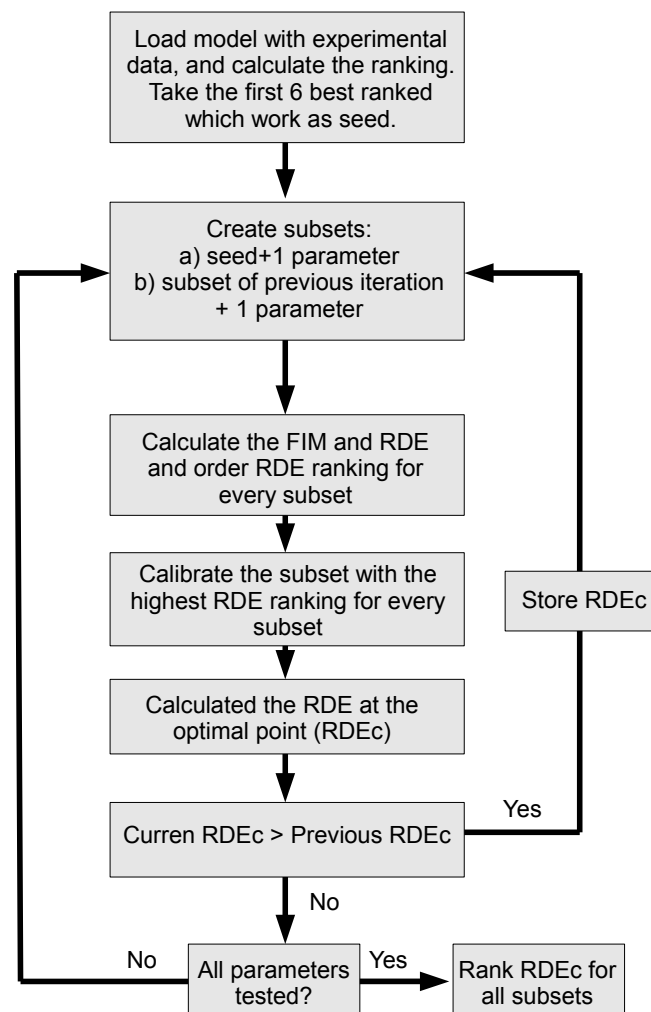


Figure 5.1: Real and simulated blood glucose level

The method described in Machada et. al. (2008)[31] is an algorithm, where the RDE-criterion is used in a systematic procedure to define the dimension of the parameter subset. The procedure was made in order to find a suitable parameter subset from a number of current of parameters. The procedure is based on the RDE criterion, and is illustrated in figure 5.1. The overall sensitivity is calculated for a certain experiment. Then, the first half of with the largest overall sensitivity is chosen, where each parameter works as a "seed" which will make the subset grow. The FIM and RDE criterion is calculated for the seed plus one parameter. When every combinations the seed and the different parameters are calculated, the RDE is sorted. The model is calibrated using real data for the subset with the largest RDE. Then, RDE is calculated in the optimal point, which is now called RDE_c . If the current RDE_c is larger than the previous, the model is updated with the calibrated values. Then, a new parameter is added to the subset, and a new iteration is started. The subset with the largest RDE_c is a subset which is able to provide a good fitting to the available experimental data [31].

5.1.1 Parameter estimation methods

A general framework for parameter estimation, or calibration, is to estimate the parameters in the model given experimental data. However, parameter estimation in nonlinear models is known to be difficult [34], where the problem is not fitting the data, but rather the ability of the model to make predictions under conditions different from the ones used in the fitting. Most current methods for parameter estimation, are to formulate the parameter estimation problem as a nonlinear optimization problem with constraints. The objective function of the optimization is defined as the discrepancy between model prediction with estimated parameters, and the experimental data. Various optimization methods have been used to solve the formulated nonlinear dynamic optimization problem [34].

The parameter identification can also be performed with an extended Kalman filter, and other various methods. However, the method of finding a suitable parameter subset with the RDE-criterion, is based on calibration an optimization algorithm, where the following cost function is minimized:

$$J = \sum_{k=1}^N (G_{real,k} - G_{estimated,k})^2 \quad (5.5)$$

5.1.2 Collecting glucose data

In order to perform the algorithm, real data was needed. From the simulation in chapter 2, there was a leak of data regarding the heart rate during exercise. Therefore, in order get real experimental data, I tested myself. The total time of the test was 320 minutes, and the blood glucose was measured with a Bayer Ascensia Contour blood glucose meter every 10 minutes. I started in fasting state, and then a meal of 70 grams carbohydrates was taken between $t=11$ and $t=14$. At $t=162$, a 25 minutes exercise session started on a cross trainer. The heart rate was measured every minute.

Between $t=213$ and $t=214$ a meal of 25 grams of carbohydrates were taken. A plot of the real and estimated data is shown in figure 5.2.

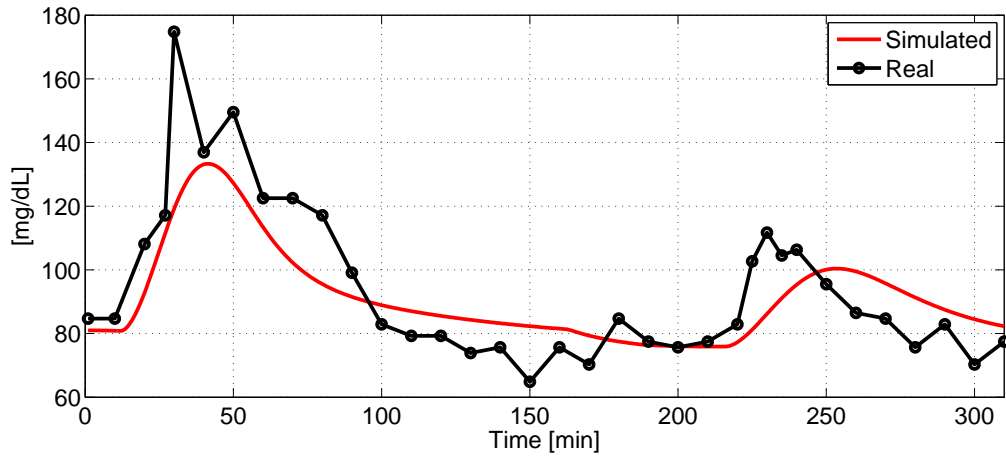


Figure 5.2: Real and simulated blood glucose level

It was shown that the parameters in the gut submodel stopped influencing the glucose output about 150 minutes after a meal. Therefore, the exercise session in the test was also chosen to start about 150 minutes after the meal. It was assumed that the ability of identify the gut parameters would increase when the model was not affected by the parameters in the exercise model. A certain time after the exercise, a meal was taken. It was assumed that the meal might show the increase in insulin sensitivity caused by the state Z .

As we can see from the plot, the model is roughly able to follow the real glucose measurements. However, it seems like the model expects a certain decrease in blood glucose during the exercise session. From the glucose measurements, there is no significant sign of any decrease in the blood glucose level during exercise.

5.1.3 RDE algorithm for the glucose model

Because the algorithm is not that computational demanding, parameters T_i and T_{ex} were also regarded, even though it was not expected that it would cause any difference in the results. Hence, the 12 parameters used in the sensitivity analysis, as shown in 4.18, were regarded. In order to find the "seeds" for the parameter subset, the overall sensitivity was calculated, and can be seen in table 5.1. The six parameters with the highest ranking were β , α , f , k_{abs} , p_1 and p_3 , and were therefore used as seed. Subsets were found corresponding to all available glucose measurement, which corresponds to a glucose measurement every 10 minutes. The result are shown in table

Table 5.1: Overall sensitivity of parameters

p_1	p_2	p_3	$1/T_d$	α	β	a	k_{abs}	k_{emp}	T_i	f	T_{ex}
36.48	0.16	0.28	0.13	154.73	399.76	2.28E-15	110.36	0.13	2.84E-4	117.07	4.73E-5

5.2, were the subsets with the highest RDE are presented in an decreasing order. This

method suggest that the parameter vector should only consist of α and f . We can see that the found optimal values sometimes varies from subset to subset. For the parameter vector $\theta = [\alpha \ f]$, the parameter α is estimated to be 60 times higher than for the parameter vector $\alpha = [p_1 \ \alpha]$.

In almost every subset, parameter α is defined at its lower bound, which correspond to 0.0097. The reason for this, is most likely due to the experimental data. The glucose measurements shown in figure 5.2 shows no reduction in the glucose level during exercise, while the sensitivity analysis showed that both α and β only have a huge influence on the glucose output during exercise. Because the exercise does not seem to affect the glucose output in the experiment, α are estimated to be small in order to fit the experimental data. For the plot 5.2, a small α as possible will reduce the negative peak during exercise. With no variation in the glucose output during exercise, the estimation of parameter α will not be possible.

Table 5.2: RDE results

Seed	Parameter vector	Optimized values	RDE_c
f	$[\alpha \ f]$	0.5870, 1.8155	0.1563
α	$[p_1 \ \alpha]$	0.0084, 0.0097	0.0134
f	$[p_1 \ \alpha \ f]$	0.1073, 0.1055, 2.5120	0.0019
p_3	$[p_3 \ \alpha]$	3.26e-05, 0.0097	3.33e-06
β	$[\alpha \ \beta]$	0.0097, 0.0013	1.48e-06
p_1	$[p_1 \ 1/T_d \ \alpha]$	0.0162, 0.0324, 0.0097	4.34e-07
f	$[p_1 \ 1/T_d \ \alpha \ f]$	0.1073, 0.0425, 0.1039, 2.3848	7.60e-08
k_{abs}	$[\alpha \ k_{abs}]$	0.0097, 0.1426	3.73e-09
p_1	$[p_1 \ 1/T_d \ \alpha \ k_{emp}]$	0.0201, 0.0234, 0.0097, 0.0530	1.01e-09

Parameter f has been assigned with an optimal value of 1.1885, or higher. Because parameter f is supposed to be a number between 0 and 1 to represent the fraction of glucose appearance from the gut, this value is meaningless. In Slezak et. al.(2010) [11], the problems estimating the parameters by an optimization solver, was discussed. When the cost function is minimized, the optimization process can force the search to go to a corner of the parameter space which, while fitting the data exquisitely, results in meaningless data. This may especially happen if the model is not an accurate fit to the true process, which it rarely is [11]. The article pointed out that especially the global minimum could result in meaningless parameters in biological systems. However, finding a global solution is most likely very hard, and a local solution might be satisfactory.

Based on these results, it is not possible to draw any conclusions. The parameter vector with the highest RDE value, include one parameter with a meaningless high value and a parameter which is most likely non-identifiable from the experimental data. If parameter f had upper bound equal to 1 and the experimental data was more informative, perhaps this would no longer be a suitable parameter vector. The big deviations in the calculated values and the values from the literature, is most likely due to lack of information in the experimental data. This may indicate that collecting enough informative data from experiments, might be challenging. Even with a moderate exercise session, it was not possible to see any reduction in the

blood glucose. Perhaps the exercise session should have started when the blood glucose level was higher, in order to see if the level would reduce.

5.2 Optimal experimental design

As we saw in the previous section, we was not able to identify parameters α and β . Was this due to the experimental setup, or is it practically impossible to identify these parameters without clamp techniques? What should be done in order to increase the identifiability? To answer these questions we may need to perform an optimal experiment.

We have seen that the identification properties depends on the performed experiment, and the resulting experimental data. Changing the input, the sampling time or the experimental duration, the covariance matrix will change and the system may not be identifiable. Therefore, the design of the experiment is of great importance. An optimal experiment will make the information data as rich as possible, which increase the ability to identify a unique parameter vector. The design of an identification experiment includes several choices that need to be evaluated, such as

- Which signals to measure
- Which signals to manipulate
- How much the signals should be manipulated
- Sampling time for measurements
- Duration of experiment
- Initial conditions for the states

Even though an optimal experiment design exists in theory, it might be impossible to perform in real life. Some inputs might not be able to be manipulated, and the input will have a limited amplitude. In other cases, neither the desired sampling time or experimental duration are possible. Sometimes, the experiment is possible to perform, but might be too expensive, too dangerous or in conflict with ethical norms. The optimal experiment is the most optimal experiment in the feasible region defined by these constraints.

Our experiment is supposed to be performed on a human being, which is either healthy or a diabetic. For a healthy person, the experiment involves measuring the blood glucose, while the manipulated variables are given by the input vector $u = [u_{meal} \ Y]$. This means that the person need to be physical active and have an intake of carbohydrates during the experiment. For a diabetic person, insulin can also be injected, which corresponds to the input vector $u = [u_{meal} \ u_{ins} \ Y]$.

In our case, there is obviously limitations in how the experiment can be performed. It is an upper limit in how much carbohydrate that can possibly be eaten during a certain time, and upper limit in how high the heart rate can possibly be. A rule of thumb is that the maximal heart rate is given as $HR_{max} = 220 - age$. There is also other practical limit, such as in how long the experiment can possibly last. If the glucose measurement need to be taken by the finger pricking method, there is also a practical limit in how often this can be done. An optimal experiment may require

specific initial conditions. However, because of lack of measurements and the difficulty to achieve these conditions within great accuracy, this seem hard to perform in practice. In addition, there are other practical limitations. It is also other practical reasons, for example, it will be difficult to inject insulin, exercise and eat at the same time.

5.2.1 Numerical solution to the optimal experimental design

In order to find an optimal experiment, we need to look into optimization theory. In general, an optimization problem consists of maximizing or minimizing a function by choosing input values, and additional parameters, within an allowed set. In our case, we want to use the D-optimality criterion and minimize $\det(C)$. In order to find an optimal experiment, the problem can be described as a dynamic optimization problem. However, the dynamic optimization problem is time continuous, and can not be solved directly. In order to solve the dynamic optimization problem, we need to apply some level of discretization that converts the original continuous time problem into a discrete problem [4]. When the input is discretized, the idea is to approximate the infinite dimensional dynamic optimization problem by a finite dimensional optimization problem. This finite dimensional optimization problem can be solved as a nonlinear programming (NLP) problem.

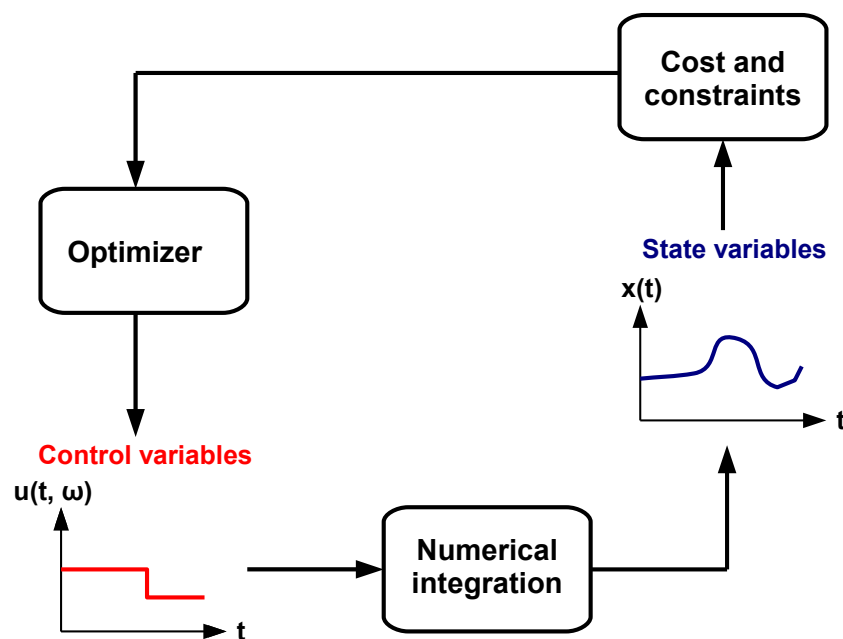


Figure 5.3: Optimal experimental design loop

In figure 5.3, we can see how we want to solve the optimality problem. The optimization starts with a guess regarding the initial state and input vector. Then, the differential equations which describe the system is solved at each iteration by a differential equation solver. At each iteration, the sensitivities and the corresponding Fisher Information matrix is calculated. This produces the value of the objective

function, which is used by a nonlinear programming solver to find the optimal control input.

Control vector parameterization

The methods that discretize the system can be divided into two categories according to the level of discretization, where partial discretization only discretize the control vector, while in full discretization both the states and control vector is discretized. For our purposes, there is no need for a full discretization. Therefore, we only want to discretize the control vector u . For partial discretization, there are several alternatives such as control vector parameterization and the multiple shooting approach. Although all of them have their own advantages and disadvantages, the CVP approach seems to be the most adequate for optimal experimental design [13]. The CVP proceeds by dividing the duration of the experiment $[t_0, t_f]$ into a number of $\rho \geq 1$ intervals.

The input can have a linear or a more complex parabolic form in each interval. However, in our case, it is natural to think of both the carbohydrate intake u_{meal} and the insulin injection u_{ins} as constant inputs in each interval. For the input Y , a linear input might seem as a natural choice because of the time it takes to reach a certain heart rate. However, to reduce the complexity, the input Y will also be seen as a constant during each interval. Because we want to set the input as a constant during each interval, the parameterization becomes very simple and is only about keeping the input constant during each interval as shown in figure 5.4

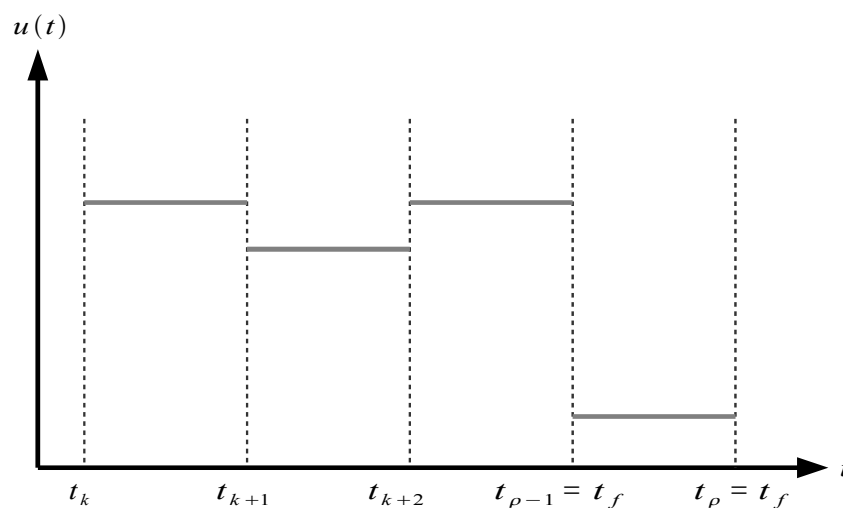


Figure 5.4: CVP and constant input

Each input u_{meal} , u_{ins} and Y will therefore be a vector which depends on the duration and number of stages ρ for each input. For example, if the experimental duration $t_f = 150$, and we want the input Y to be divided into constant workout sessions of 15 minutes, the input will be divided into $\rho = 10$ intervals, and Y will be a vector of ten elements. The time spot for when the input is able to change its value

$(t_k, t_{k+1}, \dots, t_\rho)$, is called the switching time. The simplest choice for the control switching time intervals is to choose them equal for all controls. However, in our case it might be necessary to have different switching points for every input. This because an insulin injection is done in a few second, while a carbohydrate intake might take several minutes.

Nonlinear Programming

When the control vector is discretized by control vector parameterization, the dynamic optimization problem can be approximated by solving the system as a nonlinear programming problem. The nonlinear programming problem is about minimizing the objective function $F(p)$, and can be written as [30]:

$$\min_p F(p) \quad (5.6)$$

with constraints

$$c_e(p) = 0 \quad (5.7)$$

$$c_i(p) \geq 0 \quad (5.8)$$

$$p_{i,min} \leq p_i \leq p_{i,max} \quad (5.9)$$

where $p = (p_1 \ p_2 \ \dots \ p_N)^T$ is a finite set of parameters uniquely defining the parameters to be optimized. Equation 5.7 defines a vector of equality constraints for the optimal parameter vector p , while equation 5.8 defines a vector of inequality constraints. In order to find an optimal experiment, the p -vector in the nonlinear programming problem consists of the inputs u_{meal} , u_{insa} and Y at each time step i . In addition, parameters such as the duration of the experiment can also be added.

5.2.2 Design of experiment

In order to see if it is possible to identify the parameters in the exercise submodel, an optimal experiment was designed and performed. The free variables in the optimization problem was the inputs u_{meal} and Y . The total duration of the experiment could also have been included, but it was set to 320 minutes. In order to solve the NLP problem, the Matlab optimization solver *fmincon* was used, which is able to find the minimum of a constrained, nonlinear multivariable function. The input u_{meal} was divided into intervals of 3 minutes, while Y was divided into intervals of 25 minutes. For a total time of 320 minutes, this corresponds to 107 possible u_{meal} inputs and 12 different inputs for Y . The result of the optimal experiment depends on the parameter vector. For no special reason, the parameter vector was chosen as $\theta = [p_1 \ p_2 \ 1/T_d \ \alpha \ \beta \ k_{emp}]$. This vector includes the exercise parameters which we are interested in.

The optimal experiment with only upper and lower limits for the inputs, is showed in figure 5.5, where the upper limit were 12000mg and 1.2 respectively. The glucose was supposed measured every 10 minutes. The optimal experiment requires a huge carbohydrate intake, and exercise sessions both before, during, and after the meals. This experiment will certainly give a rich output, which in turn will increase the identifiability of the parameters. However, because of the huge carbohydrate intake and as many as four exercise sessions, this experiment cannot be performed in practice

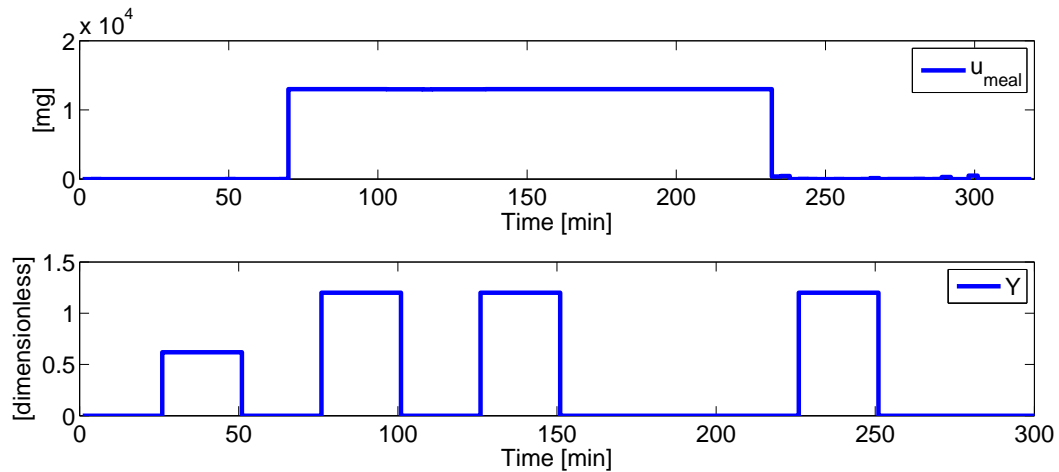


Figure 5.5: Optimal experiment

Allowing for a maximum 3 meals and 1 exercise session, where meals and exercise cannot happen simultaneously, an optimal experiment was supposed to be found. In addition, the upper limits was set to 12000 mg for the carbohydrate intake and 1.2 for the exercise input Y , which corresponds to a heart rate of 143 beats/min. However, including more constraints made the optimal solution highly dependent on the initial guess of the input. The added, nonlinear constraints tightens the feasible region, only making the it possible to find a local solution very near the initial guess. Therefore, 10 different initial guesses where chosen, and the one which showed the best performance was not seen as an optimal experiment, but as a satisfying experiment for its practical purpose.

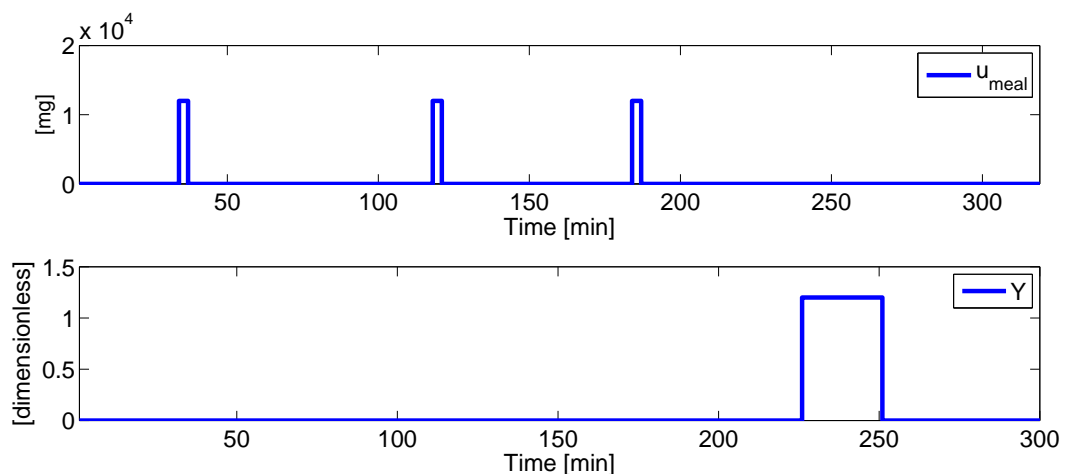


Figure 5.6: Optimal experiment with nonlinear constraints

The result is shown in figure 5.6. The three meals can be assumed to increase the ability to identify the parameters which affect the glucose output after a meal. The exercise session starts about 40 minutes after the last meal, which is the time where the blood glucose should be around its maximum. Therefore, we might be able to measure the reduction in the blood glucose due to exercise. Hence, this seem like reasonable experiment to perform.

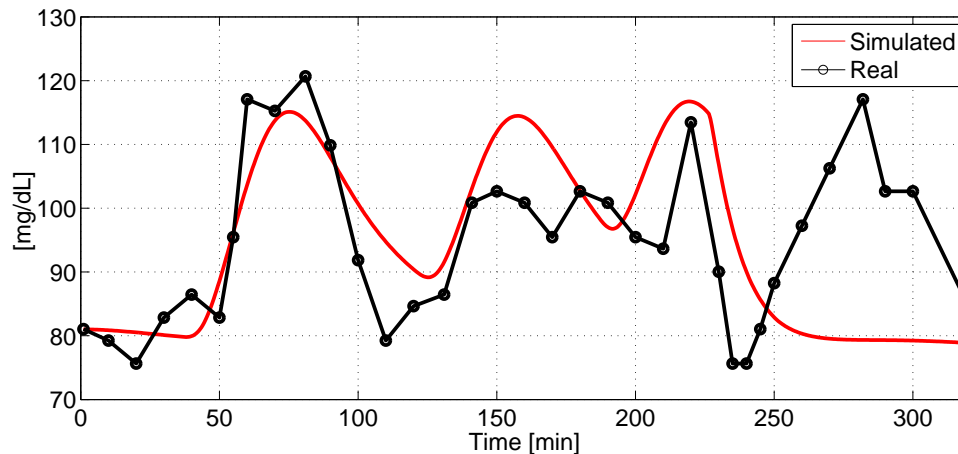


Figure 5.7: Real and simulated blood glucose level

The result from the new experiment performed on myself is shown in figure 5.7, where the blood glucose was measured every 10 minutes with the same glucose measurement meter. In order to capture the effect of exercise, the blood glucose was measured every 5 minutes during exercise. The meals were taken at $t=36$, $t=120$ and $t=186$, and contained 37 000 mg, 36 500 mg and 38 700 mg carbohydrates. The meal consisted of medium fiber crispbread with different toppings, and a small amount of banana in the last meal. The exercise started at $t=225$ and ended at $t=250$, and was done by following an aerobic program with dumbbells.

We can see the model follows roughly until half into the exercise session. The real blood glucose starts to rapidly decrease when the exercise starts, and then starts to increase after $t=240$. The simulated glucose model also starts to drop at the beginning of the exercise session, but instead of increasing it only flattens. This is true regarding to the exercise submodel, which expects a decrease during exercise, followed by increased insulin sensitivity. Hence, the exercise model seem to have some unaccounted dynamics.

In different articles, it is stated that strenuous exercise such as weight lifting, or only moderate exercise, may cause rise in the blood sugar [33]. During exercise the liver pumps out glucose, and a rate that can be very high. Sometimes the production is greater than what the body needs, which may cause the blood glucose to increase both during and after exercise. Factors such as exercise intensity, and how well trained you are, affect this process. The exercise session in my experiment was not that hard, and was interrupted for some time every 5 minutes because of the blood measurement. Still, it shows this effect, which is not considered in the glucose model. This may indicate that the glucose model is only suited for describing exercise with low intensity. Hence, one may consider to change the exercise submodel. In Dalla man et. al. (2009) [6], an exercise model was developed to take into consider-

ation the intensity of exercise. However, it does not describe the dynamics that may cause the rise in blood glucose level during or after exercise.

Because of the unmodeled dynamics, parameter identification with the collected glucose data will only result in wrong values for the identified parameters. It is not possible to find the exercise submodel parameters, and it is not possible to perform the RDE algorithm. One should consider the importance of this phenomenon.

Discussion of results and conclusion

6

6.1 Discussion

One may question the identification analysis, especially the correlation analysis. The correlation among the parameters will change when changing the input and the glucose measurement times. Therefore, it is a bit hard to draw conclusions regarding the correlation. Calculating the D-optimality value for different experiments and glucose measurement times, was supposed to give a bigger overview. However, this criterion is used in designing an optimal experiment, and it is hard to add some meaning to the D-optimality value itself. The algorithm based on the RDE criterion also failed, most likely because of lack of information in the real glucose data. However, the method may have failed even with suitable glucose data.

In order to find a suitable parameter vector, and increase the ability to estimate the parameters as accurately as possible, I think that all perhaps should be solved when designing the optimal experiment. For the glucose measurement time, the measurement time should most likely not be constant, but be placed at strategic time spots solved together with the optimal design.

6.2 Conclusion

This project was about finding a model describing the glucose metabolism model, and studying its identification properties. The model is supposed used for real-time blood glucose level prediction in a non-invasive glucose measurement device. In the literature, two certain types of glucose metabolism models were found, where the simplest minimal model described the glucose metabolism at a general level and proven to be identifiable with simple test methods. The second type of model was the maximal model, which is often complex and describes separate processes affecting the glucose level. These models often consists of a huge number of equations, and is used for research groups for simulation purposes. The parameter identification techniques are often demanding, and the parameter values found in the literature is a mean value found in a population test group.

The final model, which was chosen by Prediktor, was a minimal model where sub-models describing subcutaneous insulin injected, oral glucose intake and the effect of physical activity, were added. From real glucose test data, the simulated model

showed to roughly follow the glucose test data, and the prediction was greatly improved introducing a Kalman filter.

Because biochemical processes in the body are highly individual, and because we want the glucose model to be as accurate as possible, it is desired to calibrate the model and fit the parameters to each specific person. Therefore, the identifiability of the chosen model was studied. The calculation of the D-optimality value, showed that value of the D-optimality value depend highly on the choice of parameter vector. As expected, it was also shown that the D-optimality criterion decreases with an increase in glucose measurement sampling time. The calculated rank of the $S^T S$ matrix showed that no parameter vectors of size 9 were identifiable, and that a parameter vector of size 8 was not identifiable for all glucose measurement sampling times. This was the same in the both the case of a healthy person and a diabetic type 1 person.

Because of the small influence on the glucose output, and the strong correlations between other parameters, parameters a and T_{ex} should be found from the literature, and not be identified. On the other hand, parameters k_{abs} , f , α , β and p_1 have a huge influence on the glucose output. Based on the sensitivity and practical analysis, the parameters p_1 , p_2 , $1/T_d$, α , β and k_{emp} are not strongly correlated and have a certain effect on the blood glucose output, and seems to be suited for parameter identification. In order to pick the parameter vector in a systematic way, and too see if it was possible to find optimal values for the parameters, an algorithm based on the RDE-criterion was implemented. However, the method failed.

Collecting the last real glucose data, the data revealed that there is unmodeled dynamics in the glucose model. While the glucose model predicts that the glucose level flattens after exercise, the glucose level actually starts to increase and reach as high as 118 [mg/dL] before it decreases. The literature gives the impression of this being a common phenomenon. Hence, this perhaps makes the current model only able to predict blood glucose under low intensity exercise.

References

- [1] American Diabetes Association. Diabetes statistics, January 2013.
- [2] Marc D. Breton. Physical activity - the major unaccounted impediment to closed loop control. *Journal of Diabetes Science and Technology*, 2(1):169–174, 2008.
- [3] Robert Grover Brown and Patrick Y. C. Hwand. *Introduction to random signals and applied Kalman filtering*. John Wiley and Sons, 1997.
- [4] Arturo Cervantes and L. T. Biegler. Optimization strategies for dynamic systems, 2000.
- [5] Thomas KS Wong Joanne WY Chung Chi-Fuk So, Kup-Sze Choi. Recent advances in noninvasive glucose monitoring. *Medical Devices: Evidence and Research*, 5:45–52, 2012.
- [6] Marc D. Breton Chiara Dalla Man and Claudio Cobelli. Physical activity into the meal glucose–insulin model of type 1 diabetes: In silico studies. *Journal of Diabetes Science and Technology*, 3(1):56–67, 2009.
- [7] Robert A. Rizza Chiara Dalla Man and Claudio Cobelli. Meal simulation model of the glucose-insulin system. *IEEE transactions on biomedical engineering*, 54(10), 2007.
- [8] Lalo Magni Giuseppe De Nicolao Claudio Cobelli. Chiara Dalla Man, Giovanni Sparacino and Boris P. Kovatchev. Diabetes: Models, signals, and control. *IEEE reviews in biomedical engineering*, 2, 2009.
- [9] J. Timmer D. Faller, U. Klingmuller. Simulation methods for optimal experimental design in systems biology. *SIMULTATION*, 79(12):717–725, 2003.
- [10] Diabetes Daily. Basal/bolus therapy, April 2013.
- [11] Guillermo A. Cecchi Guillerma Marshall Gustavo Stolovitzky Diego Fernandez Slezak, Cecilia Suarez. When the optimal is not the best: Parameter estimation in complex biological models. *PloS One*, (5), 2010.
- [12] Ed Dowski. Fisher information and the cramer-rao bound, November 1995.
- [13] J.R. Banga E. Balsa-Canto, A.A. Alonso. Computational procedures for optimal experimental design in biological systems. *IET Systems Biology*, 2(3), 2007.

- [14] William J. Karnavas Eric D. Smith, Ferenc Szidarovszky and A. Terry Bahill. Sensitivity analysis, a powerful system validation technique. *The Open Cybernetics and Systemics Journal*, 2:39–56, 2008.
- [15] Julio R. Banga Eva Balsa Canto, Maria Rodriguez-Fernandez. Optimal design of dynamic experiments for improved estimation of kinetic parameters of thermal degradation. *Journal of Food Engineering*, 82:178–188, 2007.
- [16] Claudio Cobelli Gianluca Nucci. Models of subcutaneous insulin kinetics: A critical review. *Computer Methods and Programs in Biomedicine*, 62:249–257, 1999.
- [17] Ali Mohamad Hariri. Identification, state estimation, and adaptive control of type 1 diabetic patients, 2012.
- [18] John O. Holloszy. Exercise-induced increase in muscle insulin sensitivity. *Journal of Applied Physiology*, 99:338–343, 2005.
- [19] Alan S. Perelson Hongyu Miao, Xiaohua and Hulin Wu. On identifiability of nonlinear ode models and applications in viral dynamics. *SIAM Rev Soc Ind Appl Math*, 53(1):3–39, 2011.
- [20] Hope4Diabetes. Diabetes: Worldwide epidemic, January 2013.
- [21] Erik Mosekilde Iva Marija Tolic and Jeppe Sturis. Modeling the insulin-glucose feedback system: The significance of pulsatile insulin secretion. 2000.
- [22] Torkel Glad Lennart Ljung. On global identifiability for arbitrary model parametrizations. *Automatica*, 30(2):256–276, 1994.
- [23] Bhaswati Goswami Manika Saha and Ratna Ghosh. Two novel metrics for determining the tuning parameters of the kalman filter. 2013.
- [24] World Health Organization. Diabetes, January 2013.
- [25] World Health Organization. Obesity and overweight, January 2013.
- [26] C. R. Bowden R. N. Bergman, Y. Z. Ider and C. Cobelli. Quantitative estimation of insulin sensitivity. *Am J. Physiol Endocrinol Metab*, 236(E667), 1979.
- [27] Anirban Roy and Robert S. Parker. Dynamic modeling of exercise effects on plasma glucose and insulin levels. *Journal of Diabetes Science and Technology*, 1(3):338–347, 2007.
- [28] Theodore W. Zderic Lauri O Byerley Simon Schenk, Christopher J. Davidson and Edward F. Coyle. Different glycemic indexes of breakfast cereals are not due to glucose entry into blood but to glucose removal by tissue. *American Society for Clinical Nutrition*, (78):742–748, 2003.
- [29] Jay S. Skyler. *Atlas of Diabetes*. Springer, 2012.
- [30] Inge Spangelo. Trajectory optimization for vehicles using control vector parameterization and nonlinear programming, 1994.

- [31] david Gabriel javier Lafuente Juan Antonio Baeza Vinicius Cunha Machado, Gladys Tapia. Systematic identifiability study based on the fisher information matrix for reducing the number of parameters calibration of an activated sludge model. *Environmental Modelling and Software*, (24):1274–1284, 2009.
- [32] Fusheng Tang Weijiu Liu. Modeling a simplified regulatory system of blood glucose at molecular levels. *Journal of Theoretical Biology*, 252:608–620, 2008.
- [33] Rich Weil. Managing your blood glucose during exercise, June 2013.
- [34] Momiao Xiong Xiaodian Sun, Li Jin. Extended kalman filter for estimation of parameters in nonlinear state-space models of biochemical networks. *PloS One*, (11), 2008.

Appendix

Table 1: Parameter values form the litteraturel

Parameter	Value
G_b	81.0
I_b	10.0
p_1	0.0275
p_2	0.035
p_3	0.000046
T_i	0.142
V_P	117.0
V_I	11.0
T_d	10.0
R_m	80.0
C_1	120.0
a_1	10.0
k_{emp}	0.03
k_{abs}	0.06
f	0.9
HR_b	65.0
a	$(1/0.049)^4$
α	0.974
β	0.000339
T_{ex}	600.0

Table 2: Model parameter description for the minimal model

Parameter	Description	Unit
G	Plasma glucose concentration	[mg/dL]
G_b	Basal plasma glucose	[mg/dL]
X	Remote insulin action parameter	[1/min]
I	Plasma insulin concentration deviation from basal value	[mU/L]
I_b	Basak plasma insulin concentration	[mU/L]
p_1	Insulin dependent glucose removal parameter	[1/min]
p_2	Remote insulin removal rate	[1/min]
p_3	Insulin action sensivity parameter	[L/mU/min]
n	Plasma insulin decay parameter	[1/min]
R_a	The rate of glucose appearance from gut	[mg/min]
V_P	Plasma distribution space	[dL]
V_I	Insulin distribution space	[L]
U	Insulin appearance rate	[mU/min]
T_d	Time delay for subcutaneous insulin injection	[min]
S_1	Insulin in compartment one	[mU]
S_2	Insulin in compartment two	[mU]
u	Fast acting insulin injection	[mU/min]
u_b	Fast acting insulin bolus	[mU/min]
u_l	Short acting insulin	[mU/min]
R_m	Insulin production max rate	[mU/min]
C_1	The level of glucose which turn on the insulin production	[mg/dL]
a_1	Insulin production steepness parameter	[mg/dL]
Q_{sto}	Amount of glucose in the stomach	[mg]
Q_{gut}	Amount of glucose in the intestine	[mg]
k_{emp}	Rate of gastric emptying	[1/min]
k_{abs}	Rate of intestinal absorption	[1/min]
R_a	Rate of glucose appearance in plasma	[mg/min]
f	Fraction	[dimensionless]
Z	Insulin action due to exercise	[dimensionless]
Y	Energy consumption	[dimensionless]
HR	Measured heart rate	[beats/min]
HR_b	Basal heart rate	[beats/min]
a	parameter	[dimensionless]
α	Increased insulin-dependent glucose utilization parameter	[dimensionless]
β	Increased insulin-independent glucose utilization parameter	[1/min]
T_{ex}	Exercise time delay	[1/min]